(in ≥1,4 relationships) is given by E_4, where $\epsilon^* = (\epsilon_i\epsilon_k)^{1/2}$ with ϵ_i and ϵ_k representing the "hardness" of atoms i and k (kcal·mol^{-1}), $r^* = r_i + r_k$, the sum of the van der Waals radii of atoms i and k (Å), and r is the distance between the two atoms (Å). When $r^*/r > 3.311$, eq A5 reduces to $E_5 = \epsilon^*(336.176)r^*/r$ to prevent two atoms fusing when they come very close together. E_6 is the dipole interaction energy, where μ_i and μ_j are the bond moments (D) of two bonds close in space, χ is the angle between the dipoles (deg), R is the line between midpoints of the bonds, α_i and α_j are the angles (deg) between the dipole axes and the lines along which R is measured, 14.39418 converts ergs·molecule^{-1} to kcal·mol^{-1}, and D is the dielectric constant (default value = 1.5).

Registry No. Ni(porph), 15200-33-6; Fe(porph), 15213-42-0; Zn(porph), 137626-05-2; Pb(porph), 30993-25-0; $[P(TPP)(OH)_2]^+$, 87374-07-0; Ni(OEP), 24803-99-4; Fe(TPP), 16591-56-3; Zn(TPP), 14074-80-7; Pb(TPrP), 73395-80-9.

Supplementary Material Available: Listing of selected observed and MM-calculated bond lengths, bond angles, and torsional angles and a listing of modifications made to the MM2(87) program (42 pages). Ordering information is given on any current masthead page.

Theoretical Increments and Indices for Reactivity, Acidity, and Basicity within Solid-State Materials

Richard Dronskowski†

Contribution from the Department of Chemistry and Materials Science Center, Cornell University, Ithaca, New York 14853-1301. *Received November 27, 1991*

Abstract: With the aim of aiding the design of solid-state chemical syntheses, we construct some quantum mechanical indicators of reactivity, acidity, and basicity in crystal chemistry. These definitions are based on three-dimensional electronic structure calculations. After referring back to the concept of density-functional theory of Kohn and Sham and, in particular, the definition of absolute hardness due to Parr and Pearson, we first give a short overview of what is known in the field of molecular quantum chemistry. We then proceed to derive local *reactivity*, *electrophilicity* (acidity), and *nucleophilicity* (basicity) increments and indices both for atoms and bonds in any possible crystal structure. Our definitions are formulated in terms of a one-electron picture, and the first concrete calculations are performed within the framework of the semiempirical extended Hückel tight-binding method. However, the definitions are not restricted to the latter method and are quite easily generalized for ab initio numerical techniques to solve the complex eigenvalue problem in k-space. As an illustrative application, we investigate the acid–base solid-state reaction from $K_2Ti_4O_9$ to $K_2Ti_8O_{17}$. A comparison of our approach, which is suited (but not restricted) to the solid state, with another scheme from molecular orbital calculations is attempted. In detail, we (i) determine the compound's resistance to electronic attack for different electron counts, (ii) analyze all atoms with respect to their electronic reactivity, acidity, and basicity, and (iii) clearly identify the chemically most basic oxygen atom by its outstanding *atomic nucleophilicity* (basicity) *index*. In fact, the changing connectivity of this single O atom governs the structural change from $K_2Ti_4O_9$ to $K_2Ti_8O_{17}$. We perform a numerical investigation of Rouxel's hypothesis that the basicity of this particular O atom could be decreased by replacing one Ti atom by a Nb atom, and finally we elucidate the resulting changes in the electronic structure in detail.

1. Introduction

Even though the comparatively young discipline of solid-state inorganic chemistry has made great progress during the last three decades, there still seems to be a strange discrepancy in its methodology.

On one hand, modern solid-state chemistry is unthinkable without X-ray crystal structure analysis, which allows a detailed and unambiguous description of the geometry and stoichiometry of the often complex chemical structures. Therefore, one might well take the view that these huge molecules synthesized by solid-state chemists are at least as well characterized as the "typical" small molecules of solution chemistry, whose structures are often determined by various spectroscopic techniques, as well as by crystallography in the solid state.

On the other hand, a solid-state chemist engaged in generating three-dimensional periodic structures can *plan* the individual synthetical steps only in a very rudimentary way and must often rely on the classical "shake and bake" techniques.[1] While organic chemistry faces up each day to incredibly complicated organic (natural or unnatural) molecules whose syntheses are *planned step by step*, an even approximately similar strategy to retrosynthesis,[2,3] for example, seems to be out of the question for inorganic solid-state chemistry. As a matter of fact, there is no simple *Ansatz* in sight to predict nontrivial reaction paths toward *imagined* structures.

Besides the greater elemental variety of solid-state chemistry compared to organic chemistry, there is another fundamental reason for this finding. The majority of solid-state inorganic compounds is, in fact, only stable in the solid phase. This might sound trivial, but in reality it represents a singularity compared to the behavior of molecules that arise from solution chemistry. A typical giant solid-state molecule showing fascinating structural details in the crystal *decomposes* at the melting point because its chemical bonding is intimately connected to the ordered crystalline state. Thus, the confinement to a single small unit (the *molecule*), which is so successful in organic synthesis, does not seem to work. In addition, there is obviously no easy way to see or define a "functional group" in a solid-state compound, although this concept is so extremely important in organic synthesis. Even worse, one has to face the sad fact that solid-state counterparts to "functional group interconversions" or "synthons" are extremely rare.

What is retained in inorganic as well as in organic chemistry, in the solid state or in solution, is the time-honored and useful concept of acidity and basicity, except that this idea, and its

---

† Present address: Max-Planck-Institut für Festkörperforschung, Heisenbergstr. 1, 7000 Stuttgart 80, Germany.

(1) Rouxel, J. *Giving the Baker lectures at Cornell University*, 1991.

(2) Corey, E. J. *Angew. Chem.* **1991**, *103*, 469–479; *Angew. Chem., Int. Ed. Engl.* **1991**, *30*, 455–465.

(3) Warren, S. *Organic Synthesis*: *The Disconnection Approach*; John Wiley: Chichester, New York, 1982.

0002-7863/92/1514-7230$03.00/0

associated notions of electrophilicity and nucleophilicity, is not well defined in the solid state. This paper will face up to the demand for a *solid-state synthetic language* including descriptors for *reactivity*, *acidity*, and *basicity*.

2. Motivation and Starting Point

Fortunately, especially in the last decade, some solid-state syntheses of new structures give rise to the hope that the construction of a synthetic language including *reactivity* or *acidity* and *basicity* for the solid state should be worth trying, in principle.

In the solid-state chemistry of low-dimensional solids, Rouxel and others[4,5] have brought "soft chemistry" to work, incorporating (i) redox chemistry involving intercalation/deintercalation processes, (ii) acid–base reactions followed by structural recondensations, and (iii) grafting reactions using van der Waals gaps separating internal surfaces of solids.

Another example is the beautiful solid-state liquid-state donor–acceptor chemistry that has allowed infinite lattices to be "cut" into smaller pieces. As Tarascon and DiSalvo have shown, some representatives of the AMo_3X_3 structure type with A = Li, Na and X = Se, Te can be dissolved when treated with polar solvents, finally giving purely inorganic transition-metal polymer solutions.[6]

In general it should be very helpful to detect the intrinsic *reactive* or *sensitive* atomic parts of a given structure in the solid state. In other words, which sites of a structure will be most influenced by a change in the overall electronic conditions? A natural way of intellectually dividing a structure into smaller units could thereby be achieved, *without* referring back to the language of, for example, ionic or covalent bonding. There is nothing wrong with the latter, except for the tendency of each to overestimate the specific subparts they want to see (coordination polyhedra, clusters, metal–metal or metal–nonmetal bonds, and so on).

Our approach will *not* investigate the *strength* of chemical bonds in given crystal structures. Besides the fact that there are already empirical bond length–bond strength formulas available,[7-10] one might well imagine a bonding situation where a *strong* chemical bond is likely to break because of a *stronger* one formed, while a *weak* bond remains *inert* because no alternative stronger bond can be generated, for steric reasons, for instance. Again, it seems more reasonable to seek the *reactive* parts of a structure, concentrating on them while planning a synthesis. Therefore, we will try to detect and quantify, by means of electronic structure calculations, the reactive sites in a given structure. As will be seen, we believe that structures do naturally "fall apart" into sublattices of donors and acceptors.

In this paper we will set up different reactivity descriptors *for atoms and bonds* within solid-state compounds. These indicators are generated via quantum mechanical calculations of the electronic structure in the solid. The underlying concept is density-functional theory including the concept of absolute hardness, while the first calculations are performed within the framework of extended Hückel (EH) theory in its tight-binding approach.

2.1. The Hard/Soft Acid–Base Principle. There is no doubt that the formal Lewis reaction

Lewis acid + Lewis base = Lewis acid–base complex

is one of the most universal chemical reactions one can think of. The Lewis acid represents the electron acceptor, whereas the Lewis base is the electron donor. The infinite inorganic solid, of course, may be seen as the most striking example of a strong acid–base complex.

Almost 30 years ago, the Lewis theory of acids and bases was greatly augmented by the qualitative description of "hard" and "soft" acids and bases, as done by Pearson.[11-14] According to Pearson's early thesis, a "soft" acid is a big species (cation), not too highly charged, whose valence shell is easily polarizable, in contrast to a "hard" acid, which is well represented by a small and highly charged species (cation), difficult to polarize. On the other hand, a "soft" base is an easily polarizable, easily oxidizable species (anion) with a small electronegativity and low-lying orbitals. Consequently, a "hard" base is generated by a species (anion) which is difficult to polarize or oxidize, with a high electronegativity and high-lying empty orbitals. Pearson's rules that "hard" prefers "hard" and "soft" prefers "soft" have already become textbook material. It cannot be overemphasized that, in contrast to Pauling's electronegativity rule,[7] Pearson's concept manages to explain why the solid-state reaction

$$\mathrm{LiI + CsF = LiF + CsI}$$

is highly *exothermic* ($\Delta H \approx -130$ kJ/mol) on going to the *right* side which is the "soft–soft" and "hard–hard" one. As convincing as the latter example is, it is surprising that Pearson's concept has not become more popular in solid-state chemistry.

It was Klopman who set up a quantum-chemical treatment of chemical reactivity[15,16] for molecules using polyelectronic perturbation theory. His ideas could at least rationalize the initial guess of hard–hard combinations being bonded mainly by ionic forces and soft–soft combinations by mainly covalent forces. While referring to the position of the HOMO and LUMO, Klopman introduced the terms "charge-controlled" and "orbital-controlled" for hard–hard and soft–soft combinations, respectively. Moreover, he introduced reactivity scales and managed to connect them to measurable quantities such as formation enthalpies.

However, although Pearson's concept proved to be a useful one in estimating specific stabilities while combining different ions or molecules, it more or less remained an empirical criterion for 20 years. The quantification of "hard" and "soft" behavior was only set up within empirical formula schemes such as those of Drago, Wayland, and Edwards, for example. These typically include empirical "softness" and "strength" values for different molecular species, somehow linked to stability constants.[17-20]

A definite breakthrough came with the paper of Parr and Pearson in 1983 in which they simultaneously introduced *absolute electronegativity* χ and *absolute hardness* η.[21] Both were defined in terms of the ionization potential I and the electron affinity A of a system having total energy E and total electron number N according to

$$\chi = -\mu \tag{1}$$

$$= -(\partial E/\partial N)_{N^0} \tag{2}$$

$$\approx \tfrac{1}{2}(I + A) \tag{3}$$

where μ is the chemical potential and N^0 is the number of electrons within the neutral molecular species, and

$$\eta = \tfrac{1}{2}(\partial^2 E/\partial N^2)_{N^0} \tag{4}$$

$$= -\tfrac{1}{2}(\partial \chi/\partial N)_{N^0} \tag{5}$$

$$\approx \tfrac{1}{2}(I - A) \geq 0 \tag{6}$$

---

(4) Rouxel, J. *Chem. Scr.* **1988**, *28*, 33–40.

(5) Rouxel, J. *201st National Meeting of the American Chemical Society, Atlanta, GA*, Spring 1991.

(6) Tarascon, J. M.; DiSalvo, F. J.; Chen, C. H.; Carroll, P. J.; Walsh, M.; Rupp, L. *J. Solid State Chem.* **1985**, *58*, 290–300.

(7) Pauling, L. *The Nature of the Chemical Bond*, 3rd ed.; Cornell University Press: Ithaca, NY, 1960.

(8) Brown, I. D.; Wu, K. K. *Acta Cryst.* **1976**, *B32*, 1957–1959.

(9) Brown, I. D. In O'Keeffe, M., Navrotsky, A., Eds.; *Structure and Bonding in Crystals*; Academic Press: New York, 1981; Vol. II.

(10) Brown, I. D.; Altermatt, D. *Acta Cryst.* **1985**, *B41*, 244–247.

(11) Pearson, R. G. *J. Am. Chem. Soc.* **1963**, *85*, 3533–3539.

(12) Pearson, R. G. *Science* **1966**, *151*, 172–177.

(13) Pearson, R. G.; Songstad, J. *J. Am. Chem. Soc.* **1967**, *89*, 1827–1836.

(14) Pearson, R. G. *J. Chem. Educ.* **1968**, *45*, 581–587, 643–648.

(15) Klopman, G.; Hudson, R. F. *Theor. Chim. Acta* **1967**, *8*, 165–174.

(16) Klopman, G. *J. Am. Chem. Soc.* **1968**, *90*, 223–234.

(17) Ho, Tse-Lok *Hard and Soft Acids and Bases Principle in Organic Chemistry*; Academic Press: New York, 1977.

(18) Gutmann, V. *The Donor-Acceptor Approach to Molecular Interactions*; Plenum Press: New York, 1978.

(19) Jensen, W. B. *The Lewis Acid-Base Concept*; John Wiley: New York, 1980.

(20) Finston, H. L.; Rychtman, A. C. *A New View of Current Acid-Base Theories*; John Wiley: New York, 1982.

(21) Parr, R. G.; Pearson, R. G. *J. Am. Chem. Soc.* **1983**, *105*, 7512–7516.

The very last line is only valid for *stable* systems, stating that the first ionization potential is larger than the corresponding electron affinity. In fact, for atoms and molecules there are no counterexamples to eq 6 although a mathematical proof has not been given so far. For example, if eq 6 is *not* true for a system S, then 2S is unstable with respect to S^+ and S^-. Such systems would be described with a *negative* Hubbard U parameter[22] (*attractive* electron correlation).

The above statements can be exactly expressed in terms of quantum-mechanical quantities with the help of density-functional theory, i.e., as different derivatives of E versus N (see above). Thereby the "soft" and "hard" terms are given a physical basis (similar to other vivid expressions in the language of modern science, as, for example, the terms of "color", "flavor", or "charm" which are widely used in elementary particle physics).

2.2. Total Hardness and Density-Functional Theory. In contrast to traditional quantum chemical methods, density-functional (DF) theory is based on the electron density rather than on the electronic wave function ψ.[23-25] As introduced by Hohenberg, Kohn, and Sham,[26,27] DF theory explicitly includes many-particle effects that are essential for chemical bonding, and it has been proven to give an accurate description of a system's electronic ground state by Levy.[28] Within DF theory the ground state (GS) is a functional of the one-particle density $n(\bar{r})$, i.e.

$$\psi \equiv \psi\{n(\bar{r})\} \tag{7}$$

The GS energy E_0 is given as the minimum of the functional $E\{n(\bar{r})\}$ which can be separated into contributions of the kinetic energy of noninteracting electrons, classical Coulomb energy of the charge density and a functional for *exchange* and *correlation*

$$E\{n(\bar{r})\} = T\{n(\bar{r})\} + \int \mathrm{d}\bar{r} \int \mathrm{d}\bar{r}' \frac{n(\bar{r})n(\bar{r}')}{|\bar{r} - \bar{r}'|} + E^{\mathrm{xc}}\{n(\bar{r})\} + \int \mathrm{d}\bar{r}\, n(\bar{r}) v^{\mathrm{ext}}(\bar{r}) \tag{8}$$

where $v^{\mathrm{ext}}(\bar{r})$ is the Coulomb potential of the fixed nuclei. Introducing the *local-density* approximation

$$E^{\mathrm{xc}}\{n(\bar{r})\} \equiv \int \mathrm{d}\bar{r}\, n(\bar{r}) \epsilon^{\mathrm{xc}}\{n(\bar{r})\} \tag{9}$$

which is exact in the limit of slowly varying densities, the solution of the many-particle problem is reduced to the self-consistent solution of the Kohn–Sham equations

$$\{-\nabla^2 + v(\bar{r})\}\psi_j(\bar{r}) = \epsilon_j \psi_j(\bar{r}) \tag{10}$$

with an *effective* one-particle potential of the form

$$v(\bar{r}) = v^{\mathrm{ext}}(\bar{r}) + \int \frac{2n(\bar{r}')}{|\bar{r} - \bar{r}'|} \mathrm{d}\bar{r}' + v^{\mathrm{xc}}\{n(\bar{r})\} \tag{11}$$

which consists of an external potential, a Hartree potential, and a potential for exchange and correlation. Neglecting its comparatively fast computation time, by solving Hartree-like equations in a self-consistent manner, DF theory is truly size-consistent and remains an orbital theory, thereby offering advantages in interpretation compared to *configuration interaction* (CI) methods. Unfortunately, the electronic "interplay" between different configurations, which is so important in chemical reactions (transition states), is lost, and moreover, an *in principle exact* DF calculation is always only as reliable as the incorporated parametrization scheme for *exchange* and *correlation*. On the other hand, schemes well beyond the local-density approximation are already available.[29] In short, at the present time experience suggests DF calculations to be practical and accurate schemes for treating *complex* systems.

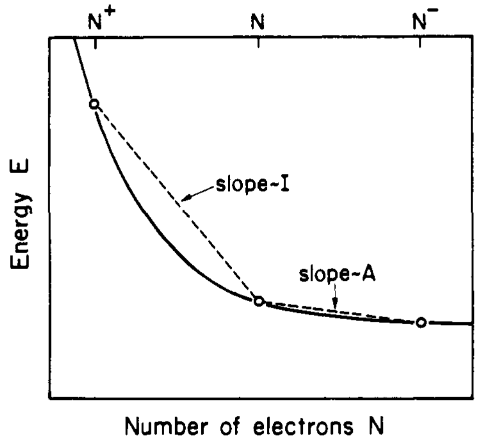

Figure 1. Total energy E of an atomic or molecular system as a function of the electron number N according to density-functional theory.[24]

From a *chemical* viewpoint, it is most interesting to investigate how the total energy E of the ground state might change with the particle (electron) number N. If one expresses E as a power series of N while keeping the potential v constant, i.e., the positions of nuclei and the atomic numbers remain fixed,

$$E = E^0 + \left(\frac{\partial E}{\partial N}\right)_{N^0} \mathrm{d}N + \frac{1}{2}\left(\frac{\partial^2 E}{\partial N^2}\right)_{N^0} \mathrm{d}N^2 + \ldots \tag{12}$$

$$= E^0 + \mu\, \mathrm{d}N + \eta\, \mathrm{d}N^2 + \ldots \tag{13}$$

to a reasonable accuracy, the change of the electronic ground state due to a change in the number of electrons is expressed by the *chemical potential* μ which equals the *slope* of the function E versus N at N^0. It measures the escaping tendency of a charged particle and, as a Lagrange multiplier, it plays a similar role within DF theory as the energy plays in the Ritz variational principle of wave-function theory. As shown in Figure 1, which gives an atom's or molecule's E versus N function in a schematical way, the slope of this function can be easily approximated by taking the arithmetic average of the slope on the "left" side (equal to the negative ionization potential I) and the slope on the "right" side (equal to the negative electron affinity A) as done in eq 3. Upon comparing Parr and Pearson's finite-difference approximation to μ with the formally identical Mulliken expression for electronegativity, it emerges that electronegativity is a concept surprisingly *consistent* and moreover *justified* within an *accurate* quantum-mechanical description of an electronic system. There is, however, a serious drawback: as pointed out early by Perdew et al.,[30] investigations on fractional electron numbers as a time average led to the conclusion that, strictly speaking, the E versus N curve is a series of *straight* line segments with slope *discontinuities* at integral N. [This does *not* necessarily hold for an atom or functional group in a molecule, and not necessarily for a species of finite T.] Consequently, the chemical potential jumps because of irregularities in the *exchange-correlation* potential. Interestingly, this fact is known as the band gap problem in calculating semiconductor band structures using DF theory. We will face it again in section 3.3.

On the other hand, the second derivative η, measuring the *curvature* of the E versus N curve, is of comparable chemical interest as it measures the electronic tendency of a system to *disproportionate* and the sensitivity of the electronegativity to

---

(22) Hubbard, J. *Proc. R. Soc. London* **1963**, *A276*, 238–257.

(23) Jones, R. O.; Gunnarsson, O. *Rev. Mod. Phys.* **1989**, *61*, 689–746.

(24) Parr, R. G.; Yang, W. *Density-Functional Theory of Atoms and Molecules*; Oxford University Press: New York, 1989.

(25) Dreizler, R. M.; Gross, E. K. U. *Density Functional Theory: An Approach to the Quantum Many-Body Problem*; Springer: Berlin, Heidelberg, New York, 1990.

(26) Hohenberg, P.; Kohn, W. *Phys. Rev.* **1964**, *136*, B864–B871.

(27) Kohn, W.; Sham, L. J. *Phys. Rev.* **1965**, *140*, A1133–A1138.

(28) Levy, M. *Proc. Natl. Acad. Sci. U.S.A.* **1979**, *76*, 6062–6065.

(29) Svane, A.; Gunnarsson, O. *Phys. Rev. B* **1988**, *37*, 9919–9922.

(30) Perdew, J. P.; Parr, R. G.; Levy, M.; Balduz, J. L., Jr. *Phys. Rev. Lett.* **1982**, *49*, 1691–1694.

change in the number of electrons. If the second derivative is greater than zero, the ground-state E is *concave upward* with changing particle number, and the system is stable against falling into charged pieces. Again the meaning of this statement can easily be visualized by looking at Figure 1. From elementary differential analysis, the finite-difference approximation for the curvature η is

$$\eta \approx \tfrac{1}{2}(E^+ + E^-) - E^0 \qquad (14)$$

This means that the system is more likely to stay at E^0 instead of breaking up into two pieces having energies of E^+ and E^-, indicated by a *positive* value of η. Therefore, it is obvious to think of the curvature value η as a *resistance* indicator of the system against any electronic (chemical) attack. Most importantly, using the finite-difference approximation which connects η to the HOMO–LUMO gap of molecules, there are no difficulties in definitions arising from those discontinuities in the E versus N curve by the ϵ^{xc} jump. Probably the first one to recognize the importance of this finite-difference approximation was Pariser who connected it to the self-repulsion integral.[31]

There are already available several tables of atoms' and small molecules' *absolute electronegativity* and *absolute hardness* values,[24,32,33] calculated using numerical estimates of electron affinities and ionization potentials from gas-phase measurements. In general, these data are in fascinating agreement with chemical knowledge. The approximate formulas

$$\Delta N = \frac{\chi_A - \chi_B}{2(\eta_A + \eta_B)} \qquad (15)$$

and

$$\Delta E = -\frac{1}{4}\frac{(\chi_A - \chi_B)^2}{\eta_A + \eta_B} \qquad (16)$$

introduced by Parr and Pearson[21] and substantially refined by Nalewajski (by incorporating electrostatic effects and resolving the "hard–hard paradox"[34]) allow the semiquantitative measure of electron transfer ΔN and energy transfer ΔE during a chemical reaction.

To further characterize the *local* consequences of total hardness at an atom within a molecule, a new quantitative scheme was proposed,[35,36] using the expressions

$$\mathrm{d}E = \mu\,\mathrm{d}N + \int n(\vec{r})\,\mathrm{d}v(\vec{r})\,\mathrm{d}\vec{r} \qquad (17)$$

$$\mathrm{d}\mu = 2\eta\,\mathrm{d}N + \int f(\vec{r})\,\mathrm{d}v(\vec{r})\,\mathrm{d}\vec{r} \qquad (18)$$

and introducing the so-called Fukui function $f(\vec{r})$ by the Maxwell relation

$$f(\vec{r}) \equiv \left[\frac{\delta\mu}{\delta v(\vec{r})}\right]_N = \left[\frac{\partial n(\vec{r})}{\partial N}\right]_v \qquad (19)$$

As is obvious from the last equation, the Fukui function is strongly related to the electron density of the *frontier orbitals* and permits one to draw contour maps for reactivity tendencies within a molecule. Moreover, Klopman's initial treatment of chemical reactivity is reinstalled. It turned out to be difficult to calculate *local hardnesses*[37,38] because of highly complicated computational expressions, and so alternative methods have been chosen to investigate local properties in molecules. The molecular *softness* S is defined[39] as half the inverse of the total hardness η

$$S = 1/2\eta \qquad (20)$$

whereas the *local softness* is given by the product of the Fukui function and molecular softness according to

$$s(\vec{r}) = Sf(\vec{r}) \qquad (21)$$

It is important to note that local softness and hardness values are not simply reciprocals of each other. The usefulness of the last definition has been shown in the course of electronegativity equalization calculations[40–42] in order to compute effective electronegativities as well as atomic charges. Typically, for the investigation of small molecules, various local softnesses are obtained with the help of so-called *condensed* Fukui functions,[43] based on gross Mulliken charges q such as

$$f_i^+ = q_i(N+1) - q_i(N) \qquad (22)$$

$$f_i^- = q_i(N) - q_i(N-1) \qquad (23)$$

$$f_i^0 = \tfrac{1}{2}[q_i(N+1) - q_i(N-1)] \qquad (24)$$

This allows the estimation of reactivities for nucleophilic, electrophilic, and radical attacks. The language of this kind of theoretical chemistry is quite mature,[24,44] and all important relations between global and local hardnesses and softnesses as well as more elaborate definitions of so-called hardness and softness *kernels* $\eta(\vec{r},\vec{r}'),s(\vec{r},\vec{r}')$, true reciprocals of each other, have already been developed. Quite recently, even higher-order derivatives were presented.[45] Applications for small molecules have been published[46,47] analyzing possible reaction paths by looking at the condensed Fukui functions. An overview of the possible calculational routes can be found in ref 48.

A slightly different approach was introduced by Nalewajski et al. who pragmatically set up an atom-in-a-molecule hardness *matrix* $\tilde{\eta}$ whose diagonal elements are given by the formula of Parr and Pearson (eq 6), whereas the nondiagonal entries are approximated semiempirically, finally giving access to normal displacement modes in electron populations. Moreover, reactive tendencies within molecules have been analyzed, especially those incorporating donor–acceptor contributions.[49,50]

Keeping all this in mind, the theoretical notation of absolute hardness and its consequences for crystal (solid-state) chemistry compared to molecular chemistry seems to have been neglected. With the exception of an early paper about structure diagrams that involves a Philips–Van Vechten-like description[51] of the solid state, on the one hand,[52] and the theoretical analysis of a bulk metal's Fukui function that comes out to be the normalized local density-of-states at the Fermi level,[39] on the other, a hardness or

---

(31) Pariser, R. *J. Chem. Phys.* **1953**, *21*, 568–569.

(32) Pearson, R. G. *Inorg. Chem.* **1988**, *27*, 734–740.

(33) Pearson, R. G. *Chem. Brit.* **1991**, 444–447.

(34) Nalewajski, R. F. *J. Am. Chem. Soc.* **1984**, *106*, 944–945.

(35) Parr, R. G.; Yang, W. *J. Am. Chem. Soc.* **1984**, *106*, 4049–4050.

(36) Yang, W.; Parr, R. G.; Pucci, R. *J. Chem. Phys.* **1984**, *81*, 2862–2863.

(37) Berkowitz, M.; Ghosh, S. K.; Parr, R. G. *J. Am. Chem. Soc.* **1985**, *107*, 6811–6814.

(38) Ghosh, S. K. *Chem. Phys. Lett.* **1990**, *172*, 77–82.

(39) Yang, W.; Parr, R. G. *Proc. Natl. Acad. Sci. U.S.A.* **1985**, *82*, 6723–6726.

(40) Yang, W.; Lee, C.; Ghosh, S. K. *J. Phys. Chem.* **1985**, *89*, 5412–5414.

(41) Mortier, W.; Ghosh, S. K.; Shankar, S. *J. Am. Chem. Soc.* **1986**, *108*, 4315–4320.

(42) Van Genechten, K. A.; Mortier, W. J.; Geerlings, P. *J. Chem. Phys.* **1987**, *86*, 5063–5071.

(43) Yang, W.; Mortier, W. J. *J. Am. Chem. Soc.* **1986**, *108*, 5708–5711.

(44) Berkowitz, M.; Parr, R. G. *J. Chem. Phys.* **1988**, *88*, 2554–2557.

(45) Fuentealba, P.; Parr, R. G. *J. Chem. Phys.* **1991**, *94*, 5559–5564.

(46) Lee, C.; Yang, W.; Parr, R. G. *J. Mol. Struct.* (*THEOCHEM*) **1988**, *163*, 305–313.

(47) Langenaeker, W.; De Decker, M.; Geerlings, P.; Raeymaekers, P. *J. Mol. Struct.* (*THEOCHEM*) **1990**, *207*, 115–130.

(48) Gãzquez, J. L.; Vela, A.; Galvãn, M. *Struct. Bonding* **1987**, *66*, 79–97.

(49) Nalewajski, R. F.; Korchowiec, J.; Zhou, Z. *Int. J. Quantum Chem.* **1988**, *22*, 349–366.

(50) Nalewajski, R. F. *Int. J. Quantum Chem.* **1991**, *40*, 265–285.

(51) Phillips, J. C.; Van Vechten, J. A. *Phys. Rev. B* **1970**, *2*, 2147–2160.

(52) Shankar, S.; Parr, R. G. *Proc. Natl. Acad. Sci. U.S.A.* **1985**, *82*, 264–266.

reactivity theory for solid-state compounds (infinite molecules) is unknown. This is very astonishing as there are already collections of empirical facts concerning the catalytic properties of solid *surfaces*, for example, which are surely a strong sign of acidic and basic material properties.[53]

The definition of the condensed Fukui function as a working tool is based on definitions of Mulliken charges, which themselves are calculated via overlap populations. In "conservative" molecular quantum mechanics, one typically deals with a well-known and still improving set of Gaussian- or Slater-type functions where the success and failure of the Mulliken overlap population scheme is well investigated. In contrast, in solid-state quantum mechanics, because of the quite different computational problems that had to be solved, a large set of most different methods was invented, typically working with sets of various basis functions such as plane waves, Gaussians, analytical atomic partial wave expansions, spherical waves, Hankel- and Bessel-type functions (often energy- and potential-dependent), and so on. To formulate a reactivity and acid–base theory that is as general as possible, we will circumvent any difficulties due to different degrees of basis set orthogonality and therefore avoid the use of overlap populations and Fukui functions.

Moreover, using such an *Ansatz* one immediately loses one of the Fukui function's limitations, namely, it being an intrinsically *relative* measure of reactivity. As already said above, local hardness $h(\vec{r})$ and local softness $s(\vec{r})$ are not true reciprocals of each other. The latter number is calculated indirectly by multiplication of S (global value) with $f(\vec{r})$ (local value). In addition, the Fukui function $f(\vec{r})$ only measures differences in electron occupations at the frontier orbitals *without* telling anything about their bonding or antibonding character. This can, of course, be done "by hand" while investigating the transparent MO order of a small molecule. In the solid state, however, the delocalization of all levels and the energy spectrum as a consequence make this a quite difficult undertaking.

From a *heuristic* standpoint, therefore, we will break down the solid-state ensemble's hardness *directly* into atomic (or bonding) contributions. As atoms condense to a solid with its given crystal structure, all absolute electronegativities equilibrate because of the governing consequences of density-functional theory. As has been pointed out earlier,[54] the electronegativity is the negative of the chemical potential, and it is the driving force of chemistry to equilibrate chemical potentials and to transfer electrons. At this point, chemical intuition asks for different chemical reactivities within the solid. Although all chemical potentials have been equilibrated, the atoms will still retain different *characteristics* while being chemically attacked. In other words, ***their resistance toward a global change in the electronic system will change from atom to atom, and that is exactly what we are going to look for.***

3. Reactivity, Acidity, and Basicity

A short theoretical outline of the concept for an isolated molecule may be taken from the Appendix. However, the following description for the solid state should be self-explanatory.

3.1. Reactivity within the Solid State. According to Bloch's theorem there is a reciprocal vector $\vec{k}$ for a wave function that fulfills Schrödinger's equation such that a translation by a real lattice vector $\vec{T}$ is equivalent to the multiplication with a phase factor

$$\phi_j(\vec{k},\vec{r} + \vec{T}) = e^{i\vec{k}\vec{T}}\phi_j(\vec{k},\vec{r}) \tag{25}$$

j is the "band index". If the Bloch function is constructed as a linear combination of atomic centered orbitals, we can write

$$\phi_j(\vec{k},\vec{r}) = \sum_T e^{i\vec{k}\vec{T}} \sum_R \sum_{\substack{\mu \\ \mu\in R}} c_{\mu j}(\vec{k})\varphi_\mu(\vec{r} - \vec{R} - \vec{T}) \tag{26}$$

where $\vec{R}$ runs over all atomic positions in the primitive unit cell and $\vec{T}$ over all its translations.

Consequently, the important difference between the molecular and the solid-state case is that we have a spectrum of different states in energy which vary with k, in contrast to the discrete energy levels of the molecule. Therefore, a well-suited description is an energy-resolved k-dependent (spectral) density-of-states matrix, here restricted to the non-spin-polarized case,

$$P_{\mu\nu}(\epsilon,\vec{k}) = \sum_j n_j c^*_{\mu j}(\vec{k}) c_{\nu j}(\vec{k}) \delta(\epsilon - \epsilon_j) \tag{27}$$

The total electronic energy (equivalent to the total energy within EH theory[59,60]) up to the Fermi energy is given by

$$E = \int \mathrm{d}\vec{k} \int^{\epsilon_F} \mathrm{d}\epsilon \sum_R \sum_{\substack{\mu \\ \mu\in R}} \Big\{ h_{\mu\mu} P_{\mu\mu}(\epsilon,\vec{k}) + \sum_{R'} \sum_{\substack{\nu \\ \nu\in R'}} \mathcal{R}[h_{\mu\nu} P_{\mu\nu}(\epsilon,\vec{k})] \Big\} \tag{28}$$

$\mathcal{R}$ characterizes the real parts of the complex off-diagonal entries. To simplify the notation, we average the k-dependent density-of-states matrix over the whole Brillouin zone and get

$$\int \mathrm{d}\vec{k} P_{\mu\nu}(\epsilon,\vec{k}) = P_{\mu\nu}(\epsilon) \tag{29}$$

Thus, the total electronic energy is rewritten as

$$E = \sum_R \sum_{\substack{\mu \\ \mu\in R}} \Big\{ \int^{\epsilon_F} h_{\mu\mu} P_{\mu\mu}(\epsilon)\, \mathrm{d}\epsilon + \sum_{R'} \sum_{\substack{\nu \\ \nu\in R'}} \int^{\epsilon_F} h_{\mu\nu} \mathcal{R}[P_{\mu\nu}(\epsilon)]\, \mathrm{d}\epsilon \Big\} \tag{30}$$

assuming the exchange integrals h to be potentially energy-*dependent*. As in a molecular case, the first part of the formula is centered at the atoms R while the second part represents the bonds within the crystal. By using the three-point finite-difference approximation (eq 14) the absolute hardness of a crystal is written as

$$\eta \approx \frac{1}{2}(E^+ + E^-) - E^0 \tag{31}$$

$$\begin{aligned} \approx \frac{1}{2}\Big[& \sum_R \sum_{\substack{\mu \\ \mu\in R}} \Big\{ \int^{\epsilon_F^+} h^+_{\mu\mu} P_{\mu\mu}(\epsilon)\, \mathrm{d}\epsilon + \sum_{R'} \sum_{\substack{\nu \\ \nu\in R'}} \int^{\epsilon_F^+} h^+_{\mu\nu} \mathcal{R}[P_{\mu\nu}(\epsilon)]\, \mathrm{d}\epsilon \Big\} \\ & + \sum_R \sum_{\substack{\mu \\ \mu\in R}} \Big\{ \int^{\epsilon_F^-} h^-_{\mu\mu} P_{\mu\mu}(\epsilon)\, \mathrm{d}\epsilon + \sum_{R'} \sum_{\substack{\nu \\ \nu\in R'}} \int^{\epsilon_F^-} h^-_{\mu\nu} \mathcal{R}[P_{\mu\nu}(\epsilon)]\, \mathrm{d}\epsilon \Big\} \Big] \\ & - \sum_R \sum_{\substack{\mu \\ \mu\in R}} \Big\{ \int^{\epsilon_F^0} h^0_{\mu\mu} P_{\mu\mu}(\epsilon)\, \mathrm{d}\epsilon + \sum_{R'} \sum_{\substack{\nu \\ \nu\in R'}} \int^{\epsilon_F^0} h^0_{\mu\nu} \mathcal{R}[P_{\mu\nu}(\epsilon)]\, \mathrm{d}\epsilon \Big\} \end{aligned} \tag{32}$$

$$\begin{aligned} \approx \sum_R \sum_{\substack{\mu \\ \mu\in R}} \Bigg\{ & \frac{1}{2}\Big(\int^{\epsilon_F^+} h^+_{\mu\mu} P_{\mu\mu}(\epsilon)\, \mathrm{d}\epsilon + \int^{\epsilon_F^-} h^-_{\mu\mu} P_{\mu\mu}(\epsilon)\, \mathrm{d}\epsilon - \\ & 2\int^{\epsilon_F^0} h^0_{\mu\mu} P_{\mu\mu}(\epsilon)\, \mathrm{d}\epsilon \Big) + \sum_{R'} \sum_{\substack{\nu \\ \nu\in R'}} \frac{1}{2}\Big(\int^{\epsilon_F^+} h^+_{\mu\nu} \mathcal{R}[P_{\mu\nu}(\epsilon)]\, \mathrm{d}\epsilon + \\ & \int^{\epsilon_F^-} h^-_{\mu\nu} \mathcal{R}[P_{\mu\nu}(\epsilon)]\, \mathrm{d}\epsilon - 2\int^{\epsilon_F^0} h^0_{\mu\nu} \mathcal{R}[P_{\mu\nu}(\epsilon)]\, \mathrm{d}\epsilon \Big) \Bigg\} \end{aligned} \tag{33}$$

where the integration in energy is to be performed for the $N - 1$ case (up to ϵ_F^+), for the N case (up to ϵ_F^0), and for the $N + 1$ case (up to ϵ_F^-).

It is clear that the crystal's hardness is given as a sum[90] of what is to be defined as an *atomic reactivity increment* ξ_R

---

(53) Tanabe, K.; Misono, M.; Ono, Y.; Hattori, H. *New Solid Acids and Bases*; Elsevier Science Publishers: Amsterdam, 1989.

(54) Donnelly, R. A.; Parr, R. G. *J. Chem. Phys.* **1978**, *69*, 4431–4439.

(55) Hall, G. G. *Proc. R. Soc. London* **1952**, *A213*, 113–123.

(56) Manning, P. P. *Proc. R. Soc. London* **1955**, *A230*, 424–428.

(57) Ruedenberg, K. *Rev. Mod. Phys.* **1962**, *34*, 326–376.

(58) Koopmans, T. *Physica* **1933**, *1*, 104–113.

(59) Hoffmann, R.; Lipscomb, W. N. *J. Chem. Phys.* **1962**, *36*, 2179–2189.

(60) Hoffmann, R. *J. Chem. Phys.* **1963**, *39*, 1397–1412.

(61) Baird, N. C. *Tetrahedron* **1970**, *26*, 2185–2190.

$$\eta \equiv \sum_{R} \xi_{\mathrm{R}} \tag{34}$$

where the definition of the *absolute* atomic reactivity increment, which is an energy value measured in eV, is formulated as

$$\xi_R \equiv \sum_{\mu \in R}^{\mu} \left\{ \frac{1}{2}\left(\int^{\epsilon_\mathrm{F}^+} h_{\mu\mu}^{+} P_{\mu\mu}(\epsilon)\,\mathrm{d}\epsilon + \int^{\epsilon_\mathrm{F}^-} h_{\mu\mu}^{-} P_{\mu\mu}(\epsilon)\,\mathrm{d}\epsilon - 2\int^{\epsilon_\mathrm{F}^0} h_{\mu\mu}^{0} P_{\mu\mu}(\epsilon)\,\mathrm{d}\epsilon \right) + \sum_{R'} \sum_{\nu \in R'}^{\nu} \frac{1}{2}\left(\int^{\epsilon_\mathrm{F}^+} h_{\mu\nu}^{+} \mathcal{R}[P_{\mu\nu}(\epsilon)]\,\mathrm{d}\epsilon + \int^{\epsilon_\mathrm{F}^-} h_{\mu\nu}^{-} \mathcal{R}[P_{\mu\nu}(\epsilon)]\,\mathrm{d}\epsilon - 2\int^{\epsilon_\mathrm{F}^0} h_{\mu\nu}^{0} \mathcal{R}[P_{\mu\nu}(\epsilon)]\,\mathrm{d}\epsilon \right) \right\} \tag{35}$$

The reader might recognize that this definition of the ξ_R incorporates sums and differences of so-called atomic Hamilton populations. Compared to the common overlap population $S_{\mu\nu}P_{\mu\nu}$ which adds up to the total number of electrons if integrated over all occupied electronic states, the Hamilton population $h_{\mu\nu}P_{\mu\nu}$ adds up to the total electronic energy, as already mentioned before. Only within EH theory is there a linear relationship between them, based on the approximation of Wolfsberg and Helmholz[62]

$$h_{\mu\nu} = K\left(\frac{h_{\mu\mu} + h_{\nu\nu}}{2}\right) S_{\mu\nu} \tag{36}$$

where K is a proportionality constant of the order 1.75. Moreover, in eq 35 the Hamilton populations both combine atomic (terms 1 to 3) and bonding parts (terms 4 to 6). We could call this a *gross* increment. However, if we artificially "cut" all bonds from an atom, its atom-centered Hamilton populations will then form a *net* atomic reactivity increment:

$$\xi_{R,\mathrm{net}} \equiv \sum_{\mu \in R}^{\mu} \frac{1}{2}\left(\int^{\epsilon_\mathrm{F}^+} h_{\mu\mu}^{+} P_{\mu\mu}(\epsilon)\,\mathrm{d}\epsilon + \int^{\epsilon_\mathrm{F}^-} h_{\mu\mu}^{-} P_{\mu\mu}(\epsilon)\,\mathrm{d}\epsilon - 2\int^{\epsilon_\mathrm{F}^0} h_{\mu\mu}^{0} P_{\mu\mu}(\epsilon)\,\mathrm{d}\epsilon \right) \tag{37}$$

If we only focus on a bond's reactivity, the investigation of the absolute *bond* reactivity increment of the bond between the atoms R and R' would be of interest, and would read

$$\xi_{RR',\mathrm{bond}} \equiv \sum_{\mu \in R}^{\mu} \sum_{\nu \in R'}^{\nu} \frac{1}{2}\left(\int^{\epsilon_\mathrm{F}^+} h_{\mu\nu}^{+} \mathcal{R}[P_{\mu\nu}(\epsilon)]\,\mathrm{d}\epsilon + \int^{\epsilon_\mathrm{F}^-} h_{\mu\nu}^{-} \mathcal{R}[P_{\mu\nu}(\epsilon)]\,\mathrm{d}\epsilon - 2\int^{\epsilon_\mathrm{F}^0} h_{\mu\nu}^{0} \mathcal{R}[P_{\mu\nu}(\epsilon)]\,\mathrm{d}\epsilon \right) \tag{38}$$

The relation between the gross, net, and bond increments is simply

$$\xi_R \equiv \xi_{R,\mathrm{net}} + \sum_{R'} \xi_{RR',\mathrm{bond}} \tag{39}$$

As a measure of energy, the value of an *absolute* reactivity increment will typically lie in a range of some meV, both below and above the energy zero. *Negative* values indicate *reactive* atoms or bonds because of their task in *decreasing* the crystal's hardness. On the contrary, *positive* values can be found at *inert* parts of the structure. If one had a high computational accuracy, those values could be compared between different structures and different compounds. Additionally, for reasons of convenience we introduce the dimensionless *relative* atomic reactivity index Ξ_R, given by the expression

$$\Xi_R \equiv \frac{\xi_R - \xi_{\max}}{\xi_{\min} - \xi_{\max}} \tag{40}$$

where all indices are normalized between "0" (most inert atom) and "1" (most reactive atom), and their symbols have been taken to be upper case Greek letters instead of lower case. Because of the normalization, they are not transferable between different compounds.

To simplify the calculations we may assume the exchange integrals to be explicitly energy-*independent*. Thus the *simplified* absolute atomic reactivity increment $\tilde{\xi}_R$ will read

$$\tilde{\xi}_R = \sum_{\mu \in R}^{\mu} \left\{ \frac{1}{2} h_{\mu\mu}\left(\int^{\epsilon_\mathrm{F}^+} P_{\mu\mu}(\epsilon)\,\mathrm{d}\epsilon + \int^{\epsilon_\mathrm{F}^-} P_{\mu\mu}(\epsilon)\,\mathrm{d}\epsilon - 2\int^{\epsilon_\mathrm{F}^0} P_{\mu\mu}(\epsilon)\,\mathrm{d}\epsilon \right) + \sum_{R'} \sum_{\nu \in R'}^{\nu} \frac{1}{2} h_{\mu\nu}\left(\int^{\epsilon_\mathrm{F}^+} \mathcal{R}[P_{\mu\nu}(\epsilon)]\,\mathrm{d}\epsilon + \int^{\epsilon_\mathrm{F}^-} \mathcal{R}[P_{\mu\nu}(\epsilon)]\,\mathrm{d}\epsilon - 2\int^{\epsilon_\mathrm{F}^0} \mathcal{R}[P_{\mu\nu}(\epsilon)]\,\mathrm{d}\epsilon \right) \right\} \tag{41}$$

Introducing a "frozen band approximation" which is the solid-state analogue of Koopmans' theorem,[58] we can further simplify the integrals' differences to

$$\tilde{\xi}_R \approx \sum_{\mu \in R}^{\mu} \left\{ \frac{1}{2} h_{\mu\mu}\left(\int^{\epsilon_\mathrm{F}^+} P_{\mu\mu}(\epsilon)\,\mathrm{d}\epsilon + \int^{\epsilon_\mathrm{F}^+} P_{\mu\mu}(\epsilon)\,\mathrm{d}\epsilon + \int_{\epsilon_\mathrm{F}^+}^{\epsilon_\mathrm{F}^0} P_{\mu\mu}(\epsilon)\,\mathrm{d}\epsilon + \int_{\epsilon_\mathrm{F}^0}^{\epsilon_\mathrm{F}^-} P_{\mu\mu}(\epsilon)\,\mathrm{d}\epsilon - 2\int^{\epsilon_\mathrm{F}^+} P_{\mu\mu}(\epsilon)\,\mathrm{d}\epsilon - 2\int_{\epsilon_\mathrm{F}^+}^{\epsilon_\mathrm{F}^0} P_{\mu\mu}(\epsilon)\,\mathrm{d}\epsilon \right) + \sum_{R'} \sum_{\nu \in R'}^{\nu} \frac{1}{2} h_{\mu\nu}\left(\int^{\epsilon_\mathrm{F}^+} \mathcal{R}[P_{\mu\nu}(\epsilon)]\,\mathrm{d}\epsilon + \int^{\epsilon_\mathrm{F}^+} \mathcal{R}[\mathrm{P}_{\mu\nu}(\epsilon)]\,\mathrm{d}\epsilon + \int_{\epsilon_\mathrm{F}^+}^{\epsilon_\mathrm{F}^0} \mathcal{R}[P_{\mu\nu}(\epsilon)]\,\mathrm{d}\epsilon + \int_{\epsilon_\mathrm{F}^0}^{\epsilon_\mathrm{F}^-} \mathcal{R}[P_{\mu\nu}(\epsilon)]\,\mathrm{d}\epsilon - 2\int^{\epsilon_\mathrm{F}^+} \mathcal{R}[P_{\mu\nu}(\epsilon)]\,\mathrm{d}\epsilon - 2\int_{\epsilon_\mathrm{F}^+}^{\epsilon_\mathrm{F}^0} \mathcal{R}[P_{\mu\nu}(\epsilon)]\,\mathrm{d}\epsilon \right) \right\} \tag{42}$$

$$\approx \frac{1}{2} \sum_{\mu \in R}^{\mu} \left\{ h_{\mu\mu}\left(\int_{\epsilon_\mathrm{F}^0}^{\epsilon_\mathrm{F}^-} P_{\mu\mu}(\epsilon)\,\mathrm{d}\epsilon - \int_{\epsilon_\mathrm{F}^+}^{\epsilon_\mathrm{F}^0} P_{\mu\mu}(\epsilon)\,\mathrm{d}\epsilon \right) + \sum_{R'} \sum_{\nu \in R'}^{\nu} h_{\mu\nu}\left(\int_{\epsilon_\mathrm{F}^0}^{\epsilon_\mathrm{F}^-} \mathcal{R}[P_{\mu\nu}(\epsilon)]\,\mathrm{d}\epsilon - \int_{\epsilon_\mathrm{F}^+}^{\epsilon_\mathrm{F}^0} \mathcal{R}[\mathrm{P}_{\mu\nu}(\epsilon)]\,\mathrm{d}\epsilon \right) \right\} \tag{43}$$

This *simplified* atomic reactivity increment is closely related to the molecular one (see Appendix), replacing the single states by a state spectrum. It turns out to be a sum of (i) the product of simple EH Hamiltonians and the difference of two "on-site" electron charge densities, i.e., an energy-weighted difference of two atomic charge density differences; and (ii) the product of "bonding" exchange integrals and the difference of all "off-site" charge density differences, *while going first from* ϵ_F^0 *to* ϵ_F^- *and then from* ϵ_F^+ *to* ϵ_F^0. Simplified reactivity increments excluding bonds (net) or excluding atoms (bond) are constructed in a similar manner.

A simple graphical visualization of the increments' meaning and the underlying partitioning technique described above is depicted in Figure 2. In the picture one can find a highly schematical representation of a total energy E versus electron number N curve of a solid-state material composed of two atoms, say A and B. Using the relative energies in the scheme, AB has an absolute hardness of $\eta \approx {}^{1}/_{2}(E^{+} + E^{-}) - E^{0} = {}^{1}/_{2}(-6 - 10) + 9 = 1$ (in arbitrary energy units) which is positive since AB is chosen to be stable. The broken line separates the *gross* atomic energies of atom A (upper part) and atom B (lower part) from each other. For each electron number N, these subenergies, which include both "on-site" and "off-site" terms since they are gross values, add up to the total energy of the crystal AB. Assuming a "frozen band approximation", the gross reactivity increments are $\tilde{\xi}_\mathrm{A} = {}^{1}/_{2}(-4 - 2) + 5 = 2$ and $\tilde{\xi}_\mathrm{B} = {}^{1}/_{2}(-2 - 8) + 4 = -1$, which means that atom B turns out to be more reactive than atom A because B has the lower increment. Actually, both increments add up to the total hardness, according to $\tilde{\xi}_\mathrm{A} + \tilde{\xi}_\mathrm{B} = 2 - 1 = 1 = \eta$, as expected.

---

[62] Wolfsberg, M.; Helmholz, L. *J. Chem. Phys.* **1952**, *20*, 837–843.

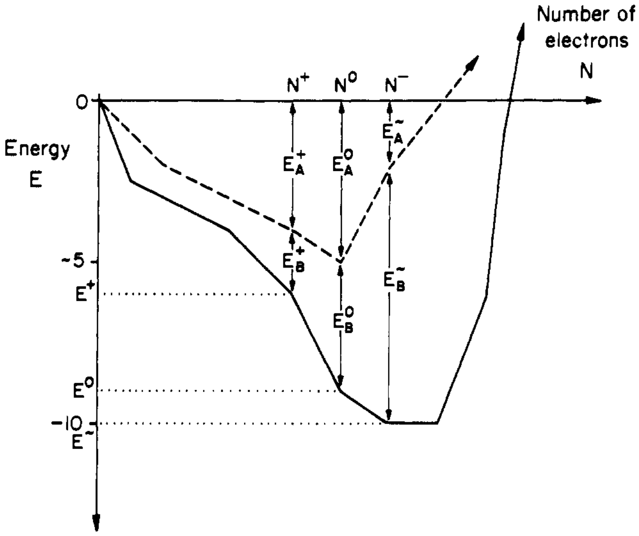

Figure 2. Schematical scheme of the total energy partitioning and its relationship with gross atomic increments of reactivity, electrophilicity, and nucleophilicity. The lower curve (bold line) represents the course of the total energy (left axis, arbitrary units) as a function of the electron number (right axis) of a solid-state material AB composed of two different atoms A and B. The total energies E^+, E^0, E^- belonging to electron numbers N^+, N^0, N^- are emphasized. The upper curve (broken line) divides the total energy into contributions of atom A (upper region) and atom B (lower region), i.e., into their atomic energies $E^+_{A,B}$, $E^0_{A,B}$, and $E^-_{A,B}$.

The corresponding definition for the *relative* simplified atomic reactivity index $\tilde{\Xi}_R$ is

$$\tilde{\Xi}_R \equiv \frac{\tilde{\xi}_R - \tilde{\xi}_{\max}}{\tilde{\xi}_{\min} - \tilde{\xi}_{\max}} \tag{44}$$

being principally the same as the one for the nonsimplified values. Trivially, atom B would have a reactivity index of $\tilde{\Xi}_B = 1$, whereas atom A would have $\tilde{\Xi}_A = 0$.

It should be emphasized that the above definitions can be used with an arbitrary basis set (plane waves, Gaussians, Hankels, etc.), although an atom-centered representation would be more comfortable because of a more convenient interpretation of the gross atomic, net atomic, and bond increments or indices. Moreover, using an atom-centered representation, the theory is applicable to *surfaces*, too. Whether a surface is computationally modelled by a cluster approach or by a two-dimensional band structure calculation (infinite slab), the partitioning of the absolute hardness into reactivity increments (eq 34) can easily be rewritten into a double-partitioning, like

$$\eta \equiv \sum_{\substack{R \\ R \in \text{surface}}} \xi_R + \sum_{\substack{R' \\ R' \in \text{bulk}}} \xi_{R'} \tag{45}$$

thus allowing the division between surface atoms and bulk atoms. A local approach to surface reactivity is installed in this way.

To summarize, we have introduced a quantitative measure of local reactivity *within* a crystal. A high positive value of ξ_R indicates stabilization of the crystal structure by making the crystal *resistant* to changes in the electron count which could occur by the attack of a reagent. A small or even negative value indicates an *intrinsic destabilizing* atom or bond.

3.2. Acidity and Basicity within the Solid State. Let us estimate what the *acid–base* property of an atom in a structure is. If one imagines an insertion reaction of a species into the sublattices of a structure or a reaction where the crystal dissolves into sublattices during its reaction with a nucleophilic or electrophilic solvent, one way of probing the acid–base behavior would be to look at the initial energy perturbations of the crystal that will arise. We therefore focus on an arbitrary reaction with a *nucleophilic reagent* (nr)

$$\text{nr} + [\text{crystal}]^0 \Leftrightarrow [\text{nr}]^{\delta+} \cdots [\text{crystal}]^{\delta-}$$

where the *crystal* reacts as an *electrophile* by accepting partial charge, and at the reaction with an *electrophilic reagent* (er)

$$\text{er} + [\text{crystal}]^0 \Leftrightarrow [\text{er}]^{\delta-} \cdots [\text{crystal}]^{\delta+}$$

where the *crystal* reacts as a *nucleophile*, i.e., donating partial charge. Dividing the arising energy perturbations into atomic contributions can be done by defining the *electrophilic energy change*, ΔE^{ele}, which is a sum over all *absolute atomic electrophilicity increments* ξ_R^{ele}, both measured in eV, given as

$$\Delta E^{\text{ele}} \approx E^- - E^0 \equiv \sum_R \xi_R^{\text{ele}} \tag{46}$$

whereas the *nucleophilic energy change*, ΔE^{nuc}, is defined as a sum over all *absolute atomic nucleophilicity increments* ξ_R^{nuc}, measured in eV, too:

$$\Delta E^{\text{nuc}} \approx E^+ - E^0 \equiv \sum_R \xi_R^{\text{nuc}} \tag{47}$$

In the example of Figure 2, the energy changes would come out to be $\Delta E^{\text{ele}} = -10 + 9 = -1$ and $\Delta E^{\text{nuc}} = -6 + 9 = 3$ (energy units).

The corresponding *relative* and dimensionless values, symbolized using upper case Greek letters again, are defined as

$$\Xi_R^{\text{ele}} \equiv \frac{\xi_R^{\text{ele}} - \xi_{\max}^{\text{ele}}}{\xi_{\min}^{\text{ele}} - \xi_{\max}^{\text{ele}}} \quad \text{and} \quad \Xi_R^{\text{nuc}} \equiv \frac{\xi_R^{\text{nuc}} - \xi_{\max}^{\text{nuc}}}{\xi_{\min}^{\text{nuc}} - \xi_{\max}^{\text{nuc}}} \tag{48}$$

for the indices of electrophilicity and nucleophilicity, respectively.

Typically, because electron density is being inserted into high-lying empty states, the *electrophilic* energy changes will come out as *negative* energies, and so do the corresponding *electrophilicity increments* (energy gain). On the other hand, because of electrons being removed from hitherto filled states, the *nucleophilic* energy changes as well as the corresponding increments will appear as *positive* energies (energy loss). The value of the nucleophilic energy change will be larger than the absolute one of the electrophilic energy change—a direct consequence of the *positive* hardness of a stable system.

In any case, *compared to the energy zero* (!), *the smaller the increments the more reactive the atoms* (*bonds*). Therefore, the electrophilic or *acidic* character of an atom (bond) will *increase* if the electrophilicity increment acquires a larger *negative* value, and atoms (bonds) will *decrease* in *acidity* if their electrophilicity increments become less *negative* or even *positive*. Consequently, the nucleophilic or *basic* character of an atom (bond) will *increase* when the nucleophilicity increment becomes less *positive* or even *negative*, and atoms (bonds) will *decrease* in *basicity* if their nucleophilicity increments become more *positive*. In short, the more negative or less positive the increment, the more reactive, acidic, or basic the atom (bond). However, for convenience the *relative* indices for electrophilicity (acidity) and nucleophilicity (basicity) are normalized in such a way that the less acidic or basic atom (bond) gets the "0" value, whereas the most acidic or basic atom (bond) can be found by looking for the "1" value.

There is a simple relation between the absolute hardness η and the electrophilic and nucleophilic energy changes, which can be derived from the formula

$$\eta \approx \tfrac{1}{2}(E^+ + E^-) - E^0 \tag{49}$$

$$\approx \tfrac{1}{2}(E^- - E^0 + E^+ - E^0) \tag{50}$$

$$\approx \tfrac{1}{2}(\Delta E^{\text{ele}} + \Delta E^{\text{nuc}}) \tag{51}$$

In fact, from the electrophilic and nucleophilic energy changes in Figure 2, one would calculate an absolute hardness of AB according to $\eta \approx {}^1/_2(\Delta E^{\text{ele}} + \Delta E^{\text{nuc}}) = {}^1/_2(-1 + 3) = 1$ which was also already found before using eq 14. Therefore, as η, ΔE^{ele}, and ΔE^{nuc} incorporate the same sum $\sum_R$ while being broken down into subcontributions, a similar formula holds for the *absolute* atomic increments

$$\xi_R = \tfrac{1}{2}(\xi_R^{\text{ele}} + \xi_R^{\text{nuc}}) \tag{52}$$

but *not* for the relative indices. By looking at eq 52, an alternative designation for the atomic *reactivity* increment could be atomic *amphoteric* increment.

The explicit formulas for ξ_R^{ele} and for ξ_R^{nuc} form only one of two parts of the absolute atomic reactivity increment. The absolute atomic *electrophilicity* increment ξ_R^{ele} is

$$\xi_R^{\text{ele}} \equiv \sum_{\substack{\mu \\ \mu\in R}} \Big\{ \Big(\int^{\epsilon_F^-} h_{\mu\mu}^- P_{\mu\mu}(\epsilon)\,\mathrm{d}\epsilon - \int^{\epsilon_F^0} h_{\mu\mu}^0 P_{\mu\mu}(\epsilon)\,\mathrm{d}\epsilon \Big) + \sum_{R'} \sum_{\substack{\nu \\ \nu\in R'}} \Big(\int^{\epsilon_F^-} h_{\mu\nu}^- \mathcal{R}[P_{\mu\nu}(\epsilon)]\,\mathrm{d}\epsilon - \int^{\epsilon_F^0} h_{\mu\nu}^0 \mathcal{R}[P_{\mu\nu}(\epsilon)]\,\mathrm{d}\epsilon \Big) \Big\} \tag{53}$$

where we assume energy-*dependent* exchange integrals h for universality. Freezing these to fixed values and using the frozen band approximation as before, we may calculate an absolute *simplified* atomic electrophilicity increment corresponding to the formula

$$\tilde{\xi}_R^{\text{ele}} = \sum_{\substack{\mu \\ \mu\in R}} \Big\{ h_{\mu\mu} \int_{\epsilon_F^0}^{\epsilon_F^-} P_{\mu\mu}(\epsilon)\,\mathrm{d}\epsilon + \sum_{R'} \sum_{\substack{\nu \\ \nu\in R'}} h_{\mu\nu} \int_{\epsilon_F^0}^{\epsilon_F^-} \mathcal{R}[P_{\mu\nu}(\epsilon)]\,\mathrm{d}\epsilon \Big\} \tag{54}$$

This expression again involves two parts that arise from products of exchange integrals with differences in electron charge densities, both "on-site" and "off-site" terms, *while going from* ϵ_F^0 to ϵ_F^-, i.e., from the neutral crystal to the slightly negatively charged one.

The definitions of the *nucleophilicity* quantities are of the same kind. For the absolute atomic *nucleophilicity* increment, we arrive at

$$\xi_R^{\text{nuc}} \equiv \sum_{\substack{\mu \\ \mu\in R}} \Big\{ \Big(\int^{\epsilon_F^+} h_{\mu\mu}^+ P_{\mu\mu}(\epsilon)\,\mathrm{d}\epsilon - \int^{\epsilon_F^0} h_{\mu\mu}^0 P_{\mu\mu}(\epsilon)\,\mathrm{d}\epsilon \Big) + \sum_{R'} \sum_{\substack{\nu \\ \nu\in R'}} \Big(\int^{\epsilon_F^+} h_{\mu\nu}^+ \mathcal{R}[P_{\mu\nu}(\epsilon)]\,\mathrm{d}\epsilon - \int^{\epsilon_F^0} h_{\mu\nu}^0 \mathcal{R}[P_{\mu\nu}(\epsilon)]\,\mathrm{d}\epsilon \Big) \Big\} \tag{55}$$

with principally energy-*dependent* exchange integrals h, whereas the *simplified* absolute value is given by

$$\tilde{\xi}_R^{\text{nuc}} = -\sum_{\substack{\mu \\ \mu\in R}} \Big\{ h_{\mu\mu} \int_{\epsilon_F^+}^{\epsilon_F^0} P_{\mu\mu}(\epsilon)\,\mathrm{d}\epsilon + \sum_{R'} \sum_{\substack{\nu \\ \nu\in R'}} h_{\mu\nu} \int_{\epsilon_F^+}^{\epsilon_F^0} \mathcal{R}[P_{\mu\nu}(\epsilon)]\,\mathrm{d}\epsilon \Big\} \tag{56}$$

Again, from Figure 2 the partitioning of the electrophilic and nucleophilic energy changes of AB can be easily visualized. For the electrophilicity increments of atoms A and B, we arrive at $\tilde{\xi}_A^{\text{ele}} = -2 + 5 = 3$ and $\tilde{\xi}_B^{\text{ele}} = -8 + 4 = -4$. Therefore, atom B is the more acidic atom since it has the lower increment. For the increments of nucleophilicity we find $\tilde{\xi}_A^{\text{nuc}} = -4 + 5 = 1$ and $\tilde{\xi}_B^{\text{nuc}} = -2 + 4 = 2$, stating that atom A is the more basic one by having the lower increment. Both the increments of electrophilicity and nucleophilicity add up to the corresponding energy changes, i.e., $\tilde{\xi}_A^{\text{ele}} + \tilde{\xi}_B^{\text{ele}} = 3 - 4 = -1 = \Delta E^{\text{ele}}$ and $\tilde{\xi}_A^{\text{nuc}} + \tilde{\xi}_B^{\text{nuc}} = 1 + 2 = 3 = \Delta E^{\text{nuc}}$.

For completeness the definitions of the *relative* simplified atomic indices are

$$\tilde{\Xi}_R^{\text{ele}} \equiv \frac{\tilde{\xi}_R^{\text{ele}} - \tilde{\xi}_{\max}^{\text{ele}}}{\tilde{\xi}_{\min}^{\text{ele}} - \tilde{\xi}_{\max}^{\text{ele}}} \quad \text{and} \quad \tilde{\Xi}_R^{\text{nuc}} \equiv \frac{\tilde{\xi}_R^{\text{nuc}} - \tilde{\xi}_{\max}^{\text{nuc}}}{\tilde{\xi}_{\min}^{\text{nuc}} - \tilde{\xi}_{\max}^{\text{nuc}}} \tag{57}$$

By inserting the results derived from Figure 2, the electrophilicity indices would simply come out to be 0 for atom A and 1 for atom B. In the case of nucleophilicity, we would find the indices to be 1 for atom A and 0 for atom B.

This concludes the definitions of the acid–base indicators for the solid state. We mention that they are *not* restricted to a specific kind of solid-state material. Whether the compound is metallic, semiconducting, or insulating is *not*, in principle, important to these definitions. A double-partitioning such as in eq 45 to distinguish between surface atoms and bulk atoms is straightforward. Thus, acidity and basicity of surface atoms may also be studied easily.

At the end of this section we would like to emphasize that the above definitions which include singly charged species do indeed correspond to the Lewis acid–base theory and its distinction from redox chemistry. Within Lewis theory this distinction is based on the truly *formal* assignment of (i) a changing *oxidation state* of an element within a compound (redox case) on the one side and (ii) the spatial redistribution of *partial charge* on atoms in a compound (acid–base case) on the other. Of course, using a quantum-mechanical language the concept of formal oxidation states can hardly survive. In fact, we may expect to find only small perturbations in the electron densities which justify our considerations, i.e., treating acidity and basicity using positively and negatively charged entities in the calculations. It should be noted that the problem of dividing acid–base from redox processes has been elucidated already more than 50 years ago in the framework of Usanovich's theory.[63] This acid–base theory explicitly includes redox chemistry as a subclass of acid–base chemistry by simply regarding the *electron* as the standard base. Unfortunately, those ideas have not become very common, probably because of language barriers, and the usual prejudices against things Russian.

3.3. Accuracy, Limitations, and Prospects. There are several theoretical aspects that have to be investigated in order to evaluate the accuracy and limitations of the reactivity and acid–base indicators presented so far.

First, the calculation of positively and negatively charged entities, assuming that no *structural* relaxation takes place, is based on a rigid band approximation. This will always lead to a small error in the total energy calculation. However, reliable computational simulation techniques for atomic displacement relaxation are only available for molecules,[64] and "straightforward solutions" for crystals are out of question.[65] Moreover, it is impossible to improve the three-point finite-difference formula by choosing smaller energy differences in the stepwise electron count since fractional occupation numbers (except in the case of an open electronic system) are in conflict with the underlying concepts of quantum mechanics.[30]

Second, the calculation of *simplified* increments for reactivity, acidity, and basicity does not take any *electronic* relaxation into account. Therefore, consequences similar to those of using Koopmans' theorem in molecular quantum mechanics, namely, too positive ionization potentials and too negative electron affinities, must arise. Fortunately, in the present case one might expect a high error cancellation rate because of the energy *difference* involved in calculating the total hardness (eq 6). Although hitherto neglected correlation effects tend to cancel relaxation errors for ionization potentials, they *add* while calculating electron affinities, and it is well known that a simple method such as EH theory does particularly badly at calculating the A's (overestimating them).

Third, the accuracy of the energy parameters within the EH tight-binding approach will always remain a problem. Although the semiempirical parameters of EH theory already carry many-particle effects into the calculations (since they are derived from experimental data), too large hardness values will appear. This can be tested only in those cases where experimental band gaps of semiconductors or insulators are available. The band gap is defined as the difference of ground-state energies

$$E^{\text{gap}} \equiv I - A \tag{58}$$

$$\equiv (E^+ - E^0) - (E^0 - E^-) \tag{59}$$

$$= 2\eta \tag{60}$$

and it is simply twice the absolute hardness. Calculations on

---

[63] Usanovich, M. *Zh. Obshch. Khim.* **1939**, *9*, 182–192.

[64] Jones, R. O. *Angew. Chem.* **1991**, *103*, 647–657; *Angew. Chem., Int. Ed. Engl.* **1991**, *30*, 630–640.

[65] Wille, L. T.; Vennik, J. *J. Phys. A* **1985**, *18*, L419–L422, L1113–L1117.

typical insulators confirm the expected error and its direction. [Using the standard values of EH theory as collected by Alvarez[66] without charge iteration, the band gaps of the highly ionic sodium chloride type compounds LiI and LiF, for example, come to around 15 and 22 eV, in contrast to the experimental values of 6 and 12 eV.] Therefore, in treating highly ionic compounds with EH theory (implicitly neglecting electrostatic contributions to the total energy), one may expect a charge iteration[67] to improve the energy parameters and hardness values significantly.

Using a more elaborate method including many-particle effects with the help of a local density or local spin-density approximation should, on the contrary, give more accurate results. Of course, it is well known that DF theory fails in calculating reliable band gaps for semiconductors. These gaps are typically *underestimated* by around 50 to 80%, while at the same time "overbonding" effects are common.[23] In the end, this is due to the possible discontinuity in the *exchange-correlation* potential. As has been shown by Perdew et al.,[68,69] the true band gap

$$E^{\text{gap}} = \epsilon^{N+1}(N) - \epsilon^{N}(N) \tag{61}$$

$$= \Delta\epsilon + \Delta \tag{62}$$

is *not* identical with the energy eigenvalue gap of the N-electron species. The failure comes from the local approximation which has its largest errors when the correlation effects are too different from the electron gas correlations. Therefore, the failures will be larger in semiconductors and insulators than in metals. However, considering the fact that absolute hardness is defined as an energy difference between *ground states of different electron number* and *not* as an excitation energy, an accurate value of η will be obtainable with three subsequent ground-state DF calculations, each for a specific total charge.

Fourth, we give the generalization of the *atomic reactivity increment* in terms of a DF ab initio framework, specifically expressed within LMTO (linear muffin-tin orbital) language in the ASA (atomic sphere approximation). The LMTO method[70-72] is the linearized version of the KKR method[73,74] where energy and potential dependent basis functions are used. One of its outstanding properties is its possible application to materials composed of atoms from any part of the periodic table. Within the ASA, where the nonspherical parts of the potentials are ignored, it is both computationally and conceptionally very efficient.

A "frozen-core approximation" (implicitely included in the EH calculations of the valence bands as well) allows the separation of the total energy into core and valence contributions. Then a crystal's valence total energy in the ASA can be expressed as

$$E^{\text{DF}}\{n(\vec{r})\} = E^{\text{one-particle}} - \sum_{R}\int^{s_R} d\vec{r}\, n_R(\vec{r})\left[\frac{1}{2}v_R^{\text{H}}(\vec{r}) + v_R^{\text{xc}}\{n(\vec{r})\}\right] + \sum_{R}\int^{s_R} d\vec{r}\, n_R(\vec{r})\,\epsilon_R^{\text{xc}}\{n(\vec{r})\} + \sum_{R}\sum_{R'}\frac{z_R z_{R'}}{|\vec{R}-\vec{R}'|} \tag{63}$$

including corrections for *exchange-correlation* and Madelung energy. The abbreviations stand for atomic sphere size s_R, Hartree and *exchange-correlation* potentials v_R^{H}, v_R^{xc}, as well as atomic charge z_R in the sphere at $\vec{R}$.[75] The "one-particle energy" $E^{\text{one-particle}}$ represents the sum of the eigenvalues which add up to the total energy only in simplified methods such as EH theory. As any of the above terms includes again the sum over all sites $\sum_R$, the DF LMTO ASA *atomic reactivity increment* reads

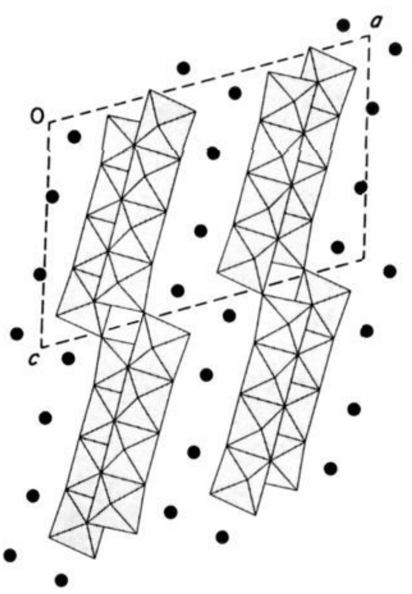

Figure 3. Projection of the crystal structure of $K_2Ti_4O_9$ along the [010] direction. The Ti–O substructure is represented with shaded octahedra, and the K atoms are given as black circles. The K atoms lie in y/b = 0 (center) and in $y/b = {}^1/_2$ (left and right). The edges of the unit cell are emphasized with broken lines.

$$\xi_R^{\text{DF}} \equiv \xi_R + \tfrac{1}{2}\{(E_R^{\text{xc}}\{\Delta n(\vec{r})\} + E_R^{\text{M}}(z_{RR'}))^{+} + (E_R^{\text{xc}}\{\Delta n(\vec{r})\} + E_R^{\text{M}}(z_{RR'}))^{-}\} - (E_R^{\text{xc}}\{\Delta n(\vec{r})\} + E_R^{\text{M}}(z_{RR'}))^{0} \tag{64}$$

where we have shortened the notation for the atomic centered correction terms of *exchange-correlation* and Madelung energy. Therefore, a generalization is easy, and the other acid–base increments change in a similar manner.

Fifth, we would like to emphasize that it should be interesting to discuss those correlation effects leading to localization phenomena such as magnetism or metal–insulator transitions[76] with the chemical language of reactivity, acidity, and basicity. Keeping in mind that the three-point finite-difference formula for the absolute hardness involves, if applied to a semiconductor or metal, an artificial insulator–metal transition, the importance of correlation (which comes into play when the bandwidth W is much smaller than the effective Coulomb interaction U) is obvious. Fortunately, the self-interaction corrected local spin-density approximation SIC-LSD[29] is believed to be able to describe these effects in a satisfying way.

Finally, Gâzquez et al. have already reported the close relationship of the spin density and the Fukui function[48] in the investigation of molecules. In particular, a linear correlation between spin-flip energy and absolute hardness was discovered. Applied to the solid state, a possible direct link between acid–base and, for example, *magnetic* behavior of atoms in crystal structures presents an interesting challenge.

4. Application

Here is a beautiful example of an acid–base solid-state synthesis. As has been shown by Rouxel in two recent publications concerned with the design and chemical reactivity of low-dimensional solids,[4,5] the topochemical reaction of $K_2Ti_4O_9$ toward $K_2Ti_8O_{17}$ that was first performed by Tournoux et al.[77] is a representative acid–base

---

(66) Alvarez, S. Universitat de Barcelona, unpublished, 1989.

(67) McGlynn, S. P.; Vanquickenborne, L. G.; Kinoshita, M.; Carroll, D. G. *Introduction to Applied Quantum Chemistry*; Holt, Rinehart and Winston: New York, 1972.

(68) Perdew, J. P.; Levy, M. *Phys. Rev. Lett.* **1983**, *51*, 1884–1887.

(69) Sham, L. J.; Schlüter, M. *Phys. Rev. Lett.* **1983**, *51*, 1888–1891.

(70) Andersen, O. K. *Phys. Rev. B* **1975**, *12*, 3060–3083.

(71) Skriver, H. L. *The LMTO Method*; Springer: Berlin, Heidelberg, New York, 1984.

(72) Andersen, O. K.; Jepsen, O.; Sob, M. In *Electronic Band Structure and Its Applications*; Yussouff, M., Ed.; Springer: Berlin, Heidelberg, New York, 1986.

(73) Korringa, J. *Physica* **1947**, *13*, 392–400.

(74) Kohn, W.; Rostoker, N. *Phys. Rev.* **1954**, *94*, 1111–1120.

(75) Andersen, O. K.; Jepsen, O.; Glötzel, D. In *Highlights of Condensed-Matter Theory*; Bassani, F., et al., Eds.; North-Holland: New York, 1985.

(76) Mott, N. F. *Metal-Insulator Transitions*; Taylor & Francis: London, New York, 1990.

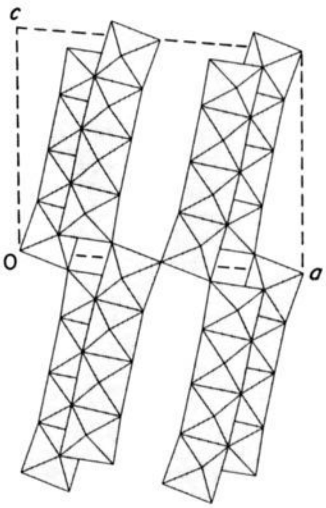

Figure 4. Projection of the Ti–O substructure of $K_2Ti_8O_{17}$ along the $[0\bar{1}0]$ direction. The Ti–O octahedra have been shaded whereas the K atoms have been omitted for clarity. The edges of the unit cell are emphasized with broken lines.

reaction of a layered solid-state material. The sheet structure of $K_2Ti_4O_9$ (Figure 3) contains zigzag Ti–O structural units, made up of four edge-sharing TiO_6 octahedra which connect to neighboring entities by sharing corner O atoms. A single Ti–O unit is furthermore linked by common edges with similar blocks above and below. There are also K^+ ions located in channel-like voids between the sheets.

Tournoux et al. discovered that the K^+ ions can be completely exchanged by H_3O^+ ions while treating $K_2Ti_4O_9$ with 3 N nitric acid at room temperature. At about 60 °C the hydrolysis product begins to emit water, accompanied by an internal protonation of the oxygen atoms, leading to –(OH) groups facing each other. At even higher temperatures further H_2O elimination may take place, leading to the sealing of neighboring Ti–O polyhedral blocks and resulting in the formation of $K_2Ti_8O_{17}$. Using slightly different conditions, a transformation to the so-called $TiO_2(B)$ structure can also be achieved. Figure 4 shows a projection of the crystal structure of $K_2Ti_8O_{17}$ (closely related to $K_3Ti_8O_{17}$).[78] The strong relationship between this structure and that of $K_2Ti_4O_9$ is immediately clear. During the hydrolysis the basic framework is *not* destroyed. The only difference lies in the additional linking of the Ti–O ribbons by a shared angular O atom. In the crystal structure of $TiO_2(B)$ (isotypical to VO_2,[79] not shown here), additional O atoms in the middle of the polyhedral unit are shared, too.

Based on these experimental facts, Rouxel came to the conclusion that, "The principle of the mechanism is based on a selective protonation of sites according to a gradation of their basicity." He further stated that, "The angular oxygen atoms represent the most basic sites [...]. They represent active sites to be protonated."[5]

We will measure the degree of basicity of all the O atoms by calculation and compare it to the available structural implications. The most basic O atom, located at the corner of the Ti–O unit, should leap to the eye upon looking at the *atomic nucleophilicity increments* or *indices*. However, if the gradients in atomic basicity should *not* turn out to be important, proton conductivity would result as a prediction. In addition, we will test Rouxel's theory on how to change the basicity of the angular O atom: "Now if we could change Ti^{4+} by Nb^{5+}, keeping the same geometry, the basicity of oxygen will considerably decrease." With this in mind, we undertood the calculations on $K_2Ti_4O_9$ and on a hypothetical "$K_2NbTi_3O_9$" with the help of the *atomic* energy partitioning technique described before. The role of *bond* reactivities and acid–base properties in different crystal structures will be the subject of forthcoming papers.[80]

Table I. K–O and Ti–O Distances (pm) up to 310 pm (K) and 220 pm (Ti) in $K_2Ti_4O_9$[a]

K(1)–O(8)	277	(2×)	K(2)–O(5)	265	(2×)
–O(9)	289	(2×)	–O(7)	287	(2×)
–O(6)	303	(2×)	–O(6)	308	(2×)
–O(6)	308	(2×)			
Ti(1)–O(9)	169		Ti(2)–O(5)	173	
–O(3)	189		–O(7)	189	
–O(8)	194		–O(2)	198	(2×)
–O(1)	196	(2×)	–O(1)	212	
–O(2)	216		–O(4)	214	
Ti(3)–O(6)	167		Ti(4)–O(8)	179	
–O(3)	197	(2×)	–O(7)	181	
–O(9)	202		–O(4)	198	(2×)
–O(5)	209		–O(2)	204	
–O(1)	219		–O(4)	208	

[a] Owing to the limited resolution of the original structure refinement[81] of $Tl_2Ti_4O_9$ (because of instrumental techniques, i.e., integrating Weissenberg film method), the standard deviations of the interatomic distances lie around 4 pm. As above distances were calculated with the use of the lattice constants of $K_2Ti_4O_9$[82] *and* the positional parameters of $Tl_2Ti_4O_9$[81] because of isotypism, the errors in the real interatomic distances could be even slightly larger.

Table II. EH Energy Parameters for $K_2Ti_4O_9$ and "$K_2NbTi_3O_9$"[a]

atom	orbital	H_{ii} (eV)	ζ_1	C_1	ζ_2	C_2
K	4s	−4.34	0.87			
	4p	−2.73	0.87			
Ti	4s	−8.97	1.08			
	4p	−5.44	0.68			
	3d	−10.81	4.55	0.4206	1.40	0.7839
Nb	5s	−10.10	1.89			
	5p	−6.86	1.85			
	4d	−12.10	4.08	0.6401	1.64	0.5516
O	2s	−32.30	2.28			
	2p	−14.80	2.28			

[a] The coefficients used in the double-ζ expansion of the *d* orbitals are designed with *C*. The ζ's are the Slater-type orbital exponents.

4.1. Calculational Details. The crystal structure of $K_2Ti_4O_9$, isostructural to $Tl_2Ti_4O_9$,[81] is characterized by a monoclinic unit cell, space group $C2/m$ (no. 12), containing four formula units, and having dimensions of a = 1825 (1) pm, b = 379.1 (1) pm, c = 1201 (1) pm, and β = 106.2 (1)°,[82] with 15 nonequivalent atoms in the cell. For the electronic structure calculations this cell was reduced to the standard primitive triclinic one in space group $P\bar{1}$ (no. 2), containing two formula units and having cell dimensions of a = 1201 pm, b = 932 pm, c = 379.1 pm, α = 101.735°, β = 90°, and γ = 106.048°. In order to avoid confusion, the atom labeling, however, was taken to be the same as in the original crystal structure communication.[81] To support the structural discussion, all interatomic distances were recalculated[83] using the original data reported, and the closest K–O and Ti–O bond lengths are given in Table I. The average Ti–O distances within the octahedral units are 193 pm at Ti(1), 197 pm at Ti(2), 199 pm at Ti(3), and 195 pm at Ti(4), in satisfying agreement with a "theoretical" Ti(+IV)–O bond length that can be calculated using Shannon's effective ionic radii.[84] [These radii are known to be *additive*, reproducing the interatomic distances if the influence of the coordination numbers (CN) is included.] Using $r_{\mathrm{Ti(+IV),\,CN=6}}$ = 60.5 pm and $r_{\mathrm{O(-II),\,CN=6}}$ = 140 pm, the expected Ti–O bond length is a little bit larger (200.5 pm) than the experimental one. Interestingly, taking the value for the Nb cation

---

(77) Marchand, R.; Brohan, L.; Tournoux, M. *Mater. Res. Bull.* **1980**, *15*, 1129–1133.

(78) Watts, J. A. *J. Solid State Chem.* **1970**, *1*, 319–325.

(79) Théobald, F.; Cabala, R.; Bernard, J. *J. Solid State Chem.* **1976**, *17*, 431–438.

(80) Dronskowski, R.; Hoffmann, R. *Inorg. Chem.*, in press.

(81) Verbaere, A.; Tournoux, M. *Bull. Soc. Chim.* **1973**, *4*, 1237–1241.

(82) Dion, M.; Piffard, Y.; Tournoux, M. *J. Inorg. Nucl. Chem.* **1978**, *40*, 917–918.

(83) Busing, W. R.; Masten, K. D.; Levy, J. A. Program ORFFE-3, ORNL-TM-306; Oak Ridge National Laboratory: Oak Ridge, TN, 1971.

(84) Shannon, R. D. *Acta Cryst.* **1976**, *A32*, 751–767.

Table III. EH Total Energies and Absolute Hardnesses of $K_2Ti_4O_9$ and "$K_2NbTi_3O_9$" for Different Valence Electron Counts[a]

compound	electrons	E (eV)	η (eV)
$[K_2Ti_4O_9]^{3+}$	69	−1381.435	
$[K_2Ti_4O_9]^{2+}$	70	−1395.993	0.012
$[K_2Ti_4O_9]^{+}$	71	−1410.527	0.016
$[K_2Ti_4O_9]^{0}$	72	−1425.030	2.545
$[K_2Ti_4O_9]^{-}$	73	−1434.442	0.110
$[K_2Ti_4O_9]^{2-}$	74	−1443.634	0.027
$[K_2Ti_4O_9]^{3-}$	75	−1452.773	
$[\text{"}K_2NbTi_3O_9\text{"}]^{+}$	72	−1429.761	
$[\text{"}K_2NbTi_3O_9\text{"}]^{0}$	73	−1440.572	0.130
$[\text{"}K_2NbTi_3O_9\text{"}]^{-}$	74	−1451.123	

[a] The electrophilic and nucleophilic energy changes of the neutral systems come to for $K_2Ti_4O_9$: $\Delta E^{ele} = -9.412$ eV, $\Delta E^{nuc} = 14.503$ eV; for "$K_2NbTi_3O_9$": $\Delta E^{ele} = -10.551$ eV, $\Delta E^{nuc} = 10.811$ eV.

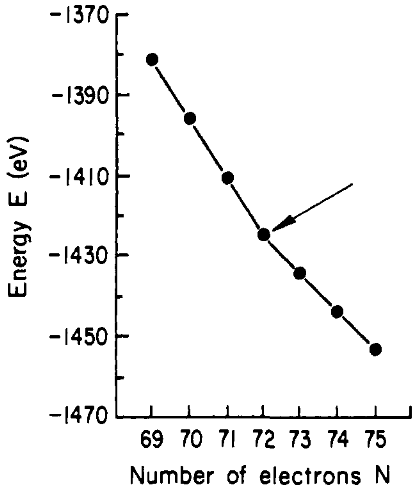

Figure 5. Total energy E of the compound $K_2Ti_4O_9$ as a function of the valence electron number N, according to the EH calculations performed. The arrow indicates the slight "bend" in the E versus N function.

$r_{Nb(+V), CN=6} = 64$ pm, the hypothetical Nb–O bond length should be only 3.5 pm larger than the Ti–O bond length. Because of this marginal difference, we decided with a good conscience to keep the geometry of the metal–nonmetal substructure *fixed* while exchanging the Ti(3) atom for a Nb atom in the model calculation of "$K_2NbTi_3O_9$".

The total number of k-points was taken to be 16, dividing the reciprocal axes into 2, 2, and 4 units, for a^*, b^*, and c^*, respectively. The extended Hückel method's H_{ii}'s were taken from the literature,[59,66,85-87] and they are given in Table II. No charge iterations were performed. Finally, total energy calculations and energy partitionings using the EH tight-binding approach[88] were performed.

4.2. Results and Discussion. 4.2.1. Absolute Hardness. The total EH energies of $K_2Ti_4O_9$ and "$K_2NbTi_3O_9$" for different electron counts may be found in Table III. A corresponding E versus N function for $K_2Ti_4O_9$ is given in Figure 5. As expected, the total energies decrease continuously with an increasing number of valence electrons. In going from the positively charged species to the neutral one (left side in Figure 5), the gain in total energy by adding one electron is always larger than the corresponding ones that arise from forming more and more negatively charged species (right side). In molecular language, the absolute values of the first ionization potential are larger than the electron affinities (*positive* hardness), typical for a *stable* system.

Table IV. Reactivity, Electrophilicity, and Nucleophilicity Increments and Indices (Gross Values) for $K_2Ti_4O_9$

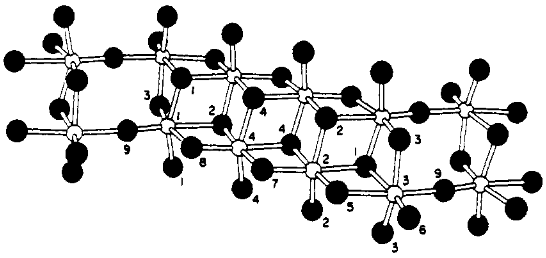

atom	$\bar{\xi}_R$ (meV)	$\bar{\xi}_R^{ele}$ (meV)	$\bar{\xi}_R^{nuc}$ (meV)	$\bar{\Xi}_R$	$\bar{\Xi}_R^{ele}$	$\bar{\Xi}_R^{nuc}$
K(1)	−10	−7	−12	0.444	0.002	0.999
K(2)	−5	7	−17	0.443	0.000	1.000
Ti(1)	−515	−1038	9	0.532	0.163	0.995
Ti(2)	−230	−486	27	0.482	0.077	0.991
Ti(3)	−3195	−6397	7	1.000	1.000	0.995
Ti(4)	−36	−113	42	0.448	0.019	0.988
O(1)	503	−153	1158	0.354	0.025	0.769
O(2)	1569	−117	3254	0.168	0.019	0.358
O(3)	−57	−281	167	0.452	0.045	0.964
O(4)	2529	−20	5078	0.000	0.004	0.000
O(5)	146	−344	635	0.416	0.055	0.872
O(6)	−63	−151	25	0.453	0.025	0.992
O(7)	945	−49	1939	0.277	0.009	0.616
O(8)	968	−64	2001	0.273	0.011	0.604
O(9)	−4	−199	191	0.443	0.032	0.959

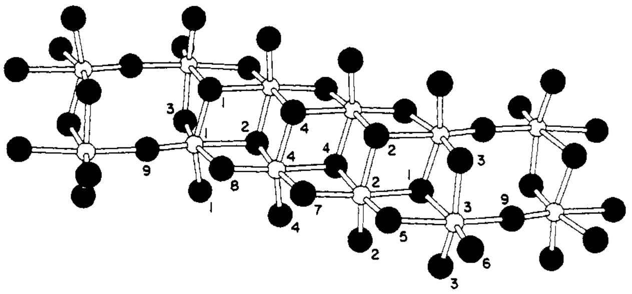

Figure 6. Perspective view of the Ti–O substructure of $K_2Ti_4O_9$, approximately along the [$\bar{1}$00] direction. The Ti atoms are given as small open circles and the O atoms as large bold circles. The atoms' labels directly correspond to Tables IV, V, VI, and VII.

The tendencies found for the different hardness values (i.e., different curvature values in Figure 5) for different electron counts (Table III) are in accord with Pearson's *maximum hardness principle*.[32] The electronic resistance of $K_2Ti_4O_9$ becomes stronger (from 0.01 eV to 0.02 eV) while approaching the neutral, stable system that has the highest hardness value of roughly 2.55 eV. By adding more electrons the hardness diminishes again (first 0.11 eV, then about 0.03 eV). For the neutral electron count quantum mechanics has *optimized* all electronic interactions (atomic "on-site" and bonding terms) so that stabilizing and destabilizing states are separated from each other as far as possible. Actually, the neutral system with its highest hardness value can be recognized by the slight "bend" in the E versus N curve in the middle of Figure 5. The other hardnesses are already so small that the remaining curve segments appear as straight lines. However, we can expect the EH hardness values to be too large compared to reality (see section 3.3). Therefore, one should keep in mind that the "bend" is already a bit overemphasized, and the schematic curve in Figure 1 is an overdramatization for pedagogical reasons.

Because of their intimate relationship, it would be interesting to compare an experimental band gap with the calculated hardness energy. Because of the high nonmetal content of $K_2Ti_4O_9$, the compound is very likely to be an insulator. Indeed, recent electrical studies show $K_2Ti_4O_9$ to be an *electronic* insulator (no band gap reported).[89,91]

---

(85) Alvarez, S.; Mota, F.; Novoa, J. *J. Am. Chem. Soc.* **1987**, *109*, 6586–6591.

(86) Lauher, J. W.; Hoffmann, R. *J. Am. Chem. Soc.* **1976**, *98*, 1729–1742.

(87) Summerville, R. H.; Hoffmann, R. *J. Am. Chem. Soc.* **1976**, *98*, 7240–7254.

(88) Hoffmann, R. *Angew. Chem.* **1987**, *99*, 871–906; *Angew. Chem., Int. Ed. Engl.* **1987**, *26*, 846–878.

Table V. Reactivity, Electrophilicity, and Nucleophilicity Increments and Indices (Net Values) for $K_2Ti_4O_9$

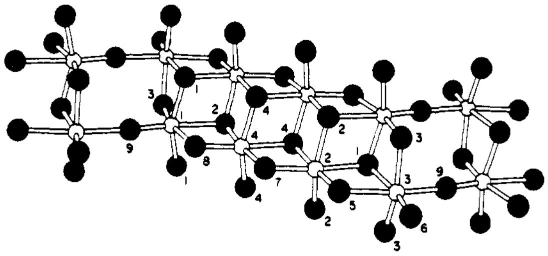

atom	$\bar{\xi}_R$ (meV)	$\bar{\xi}_R^{ele}$ (meV)	$\bar{\xi}_R^{nuc}$ (meV)	$\bar{\Xi}_R$	$\bar{\Xi}_R^{ele}$	$\bar{\Xi}_R^{nuc}$
K(1)	−1	−2	1	0.392	0.000	1.000
K(2)	−1	−2	1	0.392	0.000	1.000
Ti(1)	−658	−1318	2	0.489	0.161	1.000
Ti(2)	−283	−571	5	0.434	0.069	0.999
Ti(3)	−4092	−8188	3	1.000	1.000	1.000
Ti(4)	−59	−128	10	0.400	0.015	0.998
O(1)	402	−409	1213	0.332	0.050	0.772
O(2)	1549	−314	3411	0.161	0.038	0.359
O(3)	−285	−746	176	0.434	0.091	0.967
O(4)	2634	−57	5325	0.000	0.007	0.000
O(5)	−122	−914	670	0.410	0.111	0.874
O(6)	−193	−412	26	0.420	0.050	0.995
O(7)	953	−130	2037	0.250	0.016	0.618
O(8)	964	−173	2101	0.248	0.021	0.606
O(9)	−168	−541	204	0.417	0.066	0.962

Table VI. Reduced Fukui Functions for $K_2Ti_4O_9$

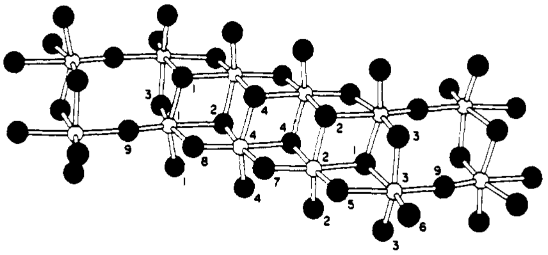

atom	f_R^0	f_R^+	f_R^-
K(1)	0.0000	−0.0008	0.0008
K(2)	0.0010	0.0008	0.0012
Ti(1)	−0.0553	−0.1100	-0.0006
Ti(2)	−0.0267	−0.0516	−0.0019
Ti(3)	−0.3402	−0.6800	−0.0005
Ti(4)	−0.0075	−0.0121	−0.0029
O(1)	−0.0480	−0.0161	−0.0799
O(2)	−0.1184	−0.0124	−0.2244
O(3)	−0.0207	−0.0298	−0.0115
O(4)	−0.1762	−0.0022	−0.3502
O(5)	−0.0402	−0.0366	−0.0438
O(6)	−0.0089	−0.0161	−0.0017
O(7)	−0.0695	−0.0052	−0.1337
O(8)	−0.0724	−0.0068	−0.1379
O(9)	−0.0172	−0.0212	−0.0132

The hypothetical compound "$K_2NbTi_3O_9$", although showing a larger total energy by about 16 eV, has a much smaller hardness value of only 0.13 eV, *smaller by a factor of 20* than the one of $K_2Ti_4O_9$. This indicates a truly greater reactivity, but not simply because of the fact that the Nb–O bonds still could readjust a little, as they are probably too small by 3 to 4 pm.

4.2.2. Reactivity. The atomic reactivity indices of $K_2Ti_4O_9$ and "$K_2NbTi_3O_9$" represent some kind of averaged measure of acid–base properties (which we will touch on in the next section). In Tables IV and V the gross and net atomic reactivity increments and indices of $K_2Ti_4O_9$ are given. For comparison we also calculated the three condensed Fukui functions (Table VI). The corresponding gross values for "$K_2NbTi_3O_9$" appear in Table VII. Figure 6 gives a "ball and stick" view of the metal–nonmetal polyhedral framework.

Table VII. Reactivity, Electrophilicity, and Nucleophilicity Increments and Indices (Gross Values) for "$K_2NbTi_3O_9$"

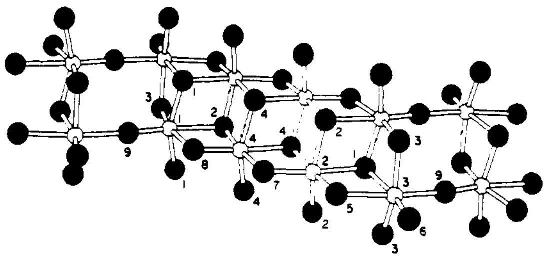

atom	$\bar{\xi}_R$ (meV)	$\bar{\xi}_R^{ele}$ (meV)	$\bar{\xi}_R^{nuc}$ (meV)	$\bar{\Xi}_R$	$\bar{\Xi}_R^{ele}$	$\bar{\Xi}_R^{nuc}$
K(1)	−3	−10	5	0.565	0.001	1.000
K(2)	−2	−8	4	0.564	0.001	1.000
Ti(1)	−4	−260	253	0.567	0.032	0.972
Ti(2)	2	−42	46	0.559	0.005	0.995
Nb	408	−8009	8825	0.000	1.000	0.000
Ti(4)	0	−2	2	0.562	0.000	1.000
O(1)	7	−65	79	0.552	0.008	0.991
O(2)	6	−25	36	0.554	0.003	0.996
O(3)	−319	−1259	621	1.000	0.157	0.930
O(4)	−1	−3	2	0.563	0.000	1.000
O(5)	34	−354	422	0.515	0.044	0.952
O(6)	−29	−186	128	0.601	0.023	0.986
O(7)	0	−2	2	0.562	0.000	1.000
O(8)	−1	−10	8	0.563	0.001	0.999
O(9)	30	−317	377	0.520	0.039	0.957

To begin with, using the gross values, both K atoms in $K_2Ti_4O_9$ show practically equal reactivity lying at an index value around 0.44. The Ti atoms follow the reactivity order

$$\text{Ti(3)} \gg \text{Ti(1)} > \text{Ti(2)} > \text{Ti(4)}$$

The Ti(3) atom which is located at the "end" of the condensed octahedra is the most reactive. The O atom reactivities span the whole spectrum from 0 to around 0.45, and the order of reactivity is

$$\text{O(6)} \geq \text{O(3)} > \text{O(9)} > \text{O(5)} > \text{O(1)} > \text{O(7)} \geq \text{O(8)} > \text{O(2)} > \text{O(4)}$$

Most interestingly, the most reactive O atoms lie around Ti(3), which is also the most reactive Ti atom! Obviously, the "last" one of the condensed Ti–O octahedra (bottom right in Figure 6) forms an "island" of reactivity. The unreactive atoms O(2) and O(4), on the contrary, are "buried" in the very middle of the polyhedral framework. We will further investigate this finding in the next section of our discussion.

The influence of all bonds within the structure can be analyzed by comparing the gross order of reactivity with the one that can be calculated from the net values of reactivity where the bonds have been artificially erased; see Table V. Concerning the K atoms, nothing important happens. This is a hint that the K atoms are inert cations whose bonding is mainly ionic in nature. For the Ti atoms the reactivity ranking becomes even *more* distinct between Ti(3) and the other three Ti atoms. Only for the O atoms does the order of reactivity show a change at the "top" where O(6) and O(3) exchange their positions. This is due to the fact that O(3) connects both Ti(1) and Ti(3), whereas O(6) is only connected to Ti(3). Switching these bonds "off" leaves less reactivity on O(6) than on O(3).

For the case of "$K_2NbTi_3O_9$" where the "alien element" Nb replaces the Ti(3) atom, we arrive at the following findings. First, the K atoms are not influenced. The Ti atoms' and the Nb atom's

---

(89) Pal, S.; Pandey, S. D.; Chand, P. *Solid State Commun.* **1989**, *69*, 1203–1206.

(90) There is a similarity between the additivity analysis presented here and a molecular additivity scheme by Harbola, Chattaraj, and Parr, in press at the *Israel Journal of Chemistry*. I am especially grateful to Professor Robert G. Parr for sending me a preprint during refereeing.

reactivities, however, have changed remarkably to

$$\mathrm{Ti(1)} \geq \mathrm{Ti(4)} \geq \mathrm{Ti(2)} \gg \mathrm{Nb}$$

Obviously, the acid–base property of the metal atom at the corner octahedron (now Nb), has undergone a conversion. Furthermore, it is noticeable that the reactivities of the O atoms (except O(3)) have now been smoothed to an average value around 0.55. We find no great diversities in the reactivities anymore, and the order reads

$$\mathrm{O(3)} \gg \mathrm{O(6)} > \mathrm{O(4)} \approx \mathrm{O(8)} \geq \mathrm{O(7)} > \mathrm{O(2)} \geq \mathrm{O(1)} \geq \mathrm{O(9)} > \mathrm{O(5)}$$

completely *rearranging* the original one. The influence of the single Nb atom on the reactivities is astonishing.

In analyzing the condensed Fukui functions f^0 for comparison, we recognize a serious drawback for their utility, since the great majority of all values are *negative*. As can be seen by careful inspection of the defining equations (22, 23, and 24), it is *inevitable* that, for example, f^0 will be *negative* for most atoms in a solid-state compound because it is a difference in particle density between the $N - 1$ particle system and the $N + 1$ particle system. Therefore, if one *assumes* that a *larger negative* value gives the *more reactive* Ti atom, the Fukui reactivity ranking *parallels* the scale of reactivity indices. In contrast to this, for the O atoms both scales run in *opposite* directions. Since the Fukui function is a *relative* scale which has to be multiplied by the absolute *softness S* to provide a semiquantitative measure, consequently, its meaning (a physical value having the dimension of *negative energy*$^{-1}$) is not easy to imagine. Similar problems *cannot* arise using the scales of *increments* and *indices*. For the remaining part of the discussion we only show the Fukui scale for the interested reader.

4.2.3. Acidity and Basicity. Although the initial intention of this investigation was based on the compound's *basic* character in a reaction with an acid, we will study its *acidity* first. From Table IV, it is not very surprising that all electrophilicity indices, except the one of Ti(3), are very small. Indeed, $K_2Ti_4O_9$ is a more basic compound, as was mentioned before. For K(1) and K(2) the $\tilde{\Xi}$ values do nearly equal 0, whereas all $\tilde{\Xi}$ values for the O atoms are below 0.06, showing them to be not acidic. It is only the Ti(3) atom that has a truly higher index of electrophilicity, as comes out from the acidity scale

$$\mathrm{Ti(3)} \gg \mathrm{Ti(1)} > \mathrm{Ti(2)} > \mathrm{Ti(4)}$$

So again Ti(3), the "corner" atom, stands out. Using the net values of Table V, which suppress chemical bonding, no significant changes can be found.

Investigating the *acidity* of the atoms in "$K_2NbTi_3O_9$", the situation is even more extreme than before. Whereas the acidic properties of K(1) and K(2) can be neglected and also the average value for the O atoms has decreased to about 0.03, the acidity of "$K_2NbTi_3O_9$" is totally based on the Nb atom—in perfect agreement with chemical intuition! Surely, a formal Nb(V) atom represents a stronger Lewis acid compared to a Ti(IV) atom. Consequently, we will expect the Nb atom to be the weakest Lewis base in this hypothetical structure. The detailed rank of acidic character for the Ti and Nb atoms is

$$\mathrm{Nb} \gg \mathrm{Ti(1)} > \mathrm{Ti(2)} > \mathrm{Ti(4)}$$

Now we finally come to the compounds' *basicity*. As far as $K_2Ti_4O_9$ is concerned, all atomic *nucleophilicity* indices in Table IV are large, indicating truly basic behavior. Surprisingly, even the K atoms show a very high degree of basicity. This is unexpected, and it means that there is still a tendency to remove charge from the K atoms. It is not clear at the moment whether this observation is of physical significance, or whether the parameters of the K atoms need modification. In general, using a semiempirical method with non-charge-iterated parameters, the comparison between *different* kinds of atoms should be made with caution.

Regarding the Ti atoms, a basicity order

$$\mathrm{Ti(3)} \geq \mathrm{Ti(1)} \geq \mathrm{Ti(2)} \geq \mathrm{Ti(4)}$$

is found. In contrast to the rank of acidities, the values found now are very homogeneous in the sense that no Ti atom is exceptional. Coming to the most interesting O atoms which lie at the reacting internal surface of $K_2Ti_4O_9$, the most distinct differences in basicity emerge. The basicity order is

$$\mathrm{O(6)} > \mathrm{O(3)} > \mathrm{O(9)} > \mathrm{O(5)} > \mathrm{O(1)} > \mathrm{O(7)} > \mathrm{O(8)} \gg \mathrm{O(2)} \gg \mathrm{O(4)}$$

being the same as the one in the reactivity section, a clear hint that the O atom reactivities run parallel to their basicities! Again, we stress that the *most basic* O atoms, namely O(6), O(3), O(9), O(5), and O(1), are surrounding the most reactive (and most acidic) Ti atom in the corner octahedron. Specifically, it is the O(6) atom with its highest $\tilde{\Xi}^{\mathrm{nuc}}$ value of 0.992 which is protonated in the acid–base reaction of Tournoux! Taking the essence of classical acid–base reactions in solutions into account, it is not surprising at all that most acidic and most basic atoms try to bond together. So what is found for Ti(3) and its nearest shell of O atoms is in nice accordance with chemical knowledge.

Furthermore, to form higher condensates like TiO_2(B), for example, a further protonation of the O atoms at the "long edge" has to take place. Indeed, the $\tilde{\Xi}^{\mathrm{nuc}}$ scale shows a continuous decrease along O(6), O(5), O(7), and O(8). On the contrary, the least basic (and least reactive) atoms O(2) and O(4) are never affected in these reactions. They are located in the inner part of the Ti–O framework and their *nucleophilicity* indices are extremely small.[92] The same conclusions, to bring the discussion of $K_2Ti_4O_9$ to an end, can be drawn from the net values, without any significant differences.

Investigating the atomic basicities within "$K_2NbTi_3O_9$", the roles of the K atoms remain unchanged. We already expected a possible small basicity for the Nb atom, and this is exactly what we find. According to

$$\mathrm{Ti(4)} \geq \mathrm{Ti(2)} > \mathrm{Ti(1)} \gg \mathrm{Nb}$$

the former order of the Ti atoms has been *inverted*, transforming the *inner* Ti atoms into the *more* basic and the *outer* Ti and Nb atoms into the *less* basic ones. In particular, the strong Lewis acid Nb(V) represents the least basic site, confirming our initial expectations.

By looking at the basicities of the O atoms,

$$\mathrm{O(4)} \approx \mathrm{O(7)} \geq \mathrm{O(8)} \geq \mathrm{O(2)} > \mathrm{O(1)} > \mathrm{O(6)} > \mathrm{O(9)} \geq \mathrm{O(5)} > \mathrm{O(3)}$$

Rouxel's initial idea has truly been proven to be right. The O(6) atom and the other O atoms at the end of the Ti–O entity have been greatly reduced in basicity, and the centers of basicity are now located mainly in the *middle* of the building block! In chemical language, this is the result of an extremely strong acid's (Nb(V)) power to weaken the basicity of its environment.

From a more physical point of view, why is there such a drastic change in the different indices upon Nb substitution? There could be at least three different reasons. First, the influence of the different spatial extent of the atomic wave functions of Nb and Ti atoms (Table II) could play a role. By looking at the coefficients of the Slater-type orbitals, the Ti atom turns out to be more diffuse than the Nb atom. Second, the differences in electronegativity ($EN_{Ti} = 1.5$, $EN_{Nb} = 1.6$)[7] will have some importance for the degree of ionicity versus covalency, and, consequently, for the order of basicities. From Table II the larger H_{ii} values for Nb than for Ti are obvious, and the stronger atomic potential of Nb stands for the greater electronegativity. And there is simply the influence of the additional electron which is brought into the structure by Nb substitution.

---

(91) Because of the high mobility of the K cations, a purely *ionic* conduction mechanism was also found at high temperatures.

(92) It is true that a protonation of the O(6) atom will also affect the electronic structure of the mid-oxygen atoms. However, here we only focus on the initial act of electronic perturbation.

We therefore undertook three total energy calculations for $K_2Ti_4O_9$ where (i) the Ti(3) atom entered the computations with atomic wave functions of Nb, i.e., having the Nb Slater-type orbital exponents; (ii) the Ti(3) atom was given the electronegativity of Nb, i.e., represented by the H_{ii} values of Nb; and (iii) the computations were performed for the pure Ti compound that had one additional negative charge, i.e., 73 instead of 72 valence electrons.

The results are given in Table VIII. Keeping in mind that the change in the absolute hardness in going from $K_2Ti_4O_9$ to "$K_2NbTi_3O_9$" turned out to be a factor of about 20, the effect of the Nb atomic functions is surprisingly small, as it leads to a decrease in η from approximately 2.55 eV to 2.36 eV. The influence of the change in electronegativity (diagonal Hamiltonian matrix elements) is slightly larger but still comparatively small since η is only decreased to about 2.09 eV. Additionally, the detailed analysis of the basicity orders of the O atoms do *not* show any significant changes if compared to the "pure" $K_2Ti_4O_9$ compound. Neither the difference in atomic wave functions nor the differences in electronegativity between Ti and Nb have a strong influence on reactivity or basicity.

However, the change due to the additional electron is tremendous. The absolute hardness is decreased to about 0.11 eV which even is below η("$K_2NbTi_3O_9$") by 20 meV, a clear hint that, in fact, the compound incorporating Nb is better suited to accomodate the additional electron. Furthermore, the order of basicity of the O atoms reads

$$\mathrm{O}(4) > \mathrm{O}(7) \geq \mathrm{O}(8) \geq \mathrm{O}(2) > \mathrm{O}(1) \approx \mathrm{O}(6) > \mathrm{O}(9) > \mathrm{O}(3) > \mathrm{O}(5)$$

nearly identical (except of the last two atoms) with the one of "$K_2NbTi_3O_9$". So what appeared to be the consequence of an "alien" element is, in the end, to a very high degree the effect of an additional electron. In molecular orbital language, this electron, which is pushing down the crystal's resistance, must be placed in an antibonding band. In fact, the total overlap populations of the Ti(3)–O bonds integrated up to the Fermi level (Figure 7) reveal that the bond strengths are sharply reduced on going past electroneutrality. While the integrated overlap populations remain mainly unchanged if the crystal's positive charge is decreased toward neutrality, an increase in negative charge weakens the Ti(3)–O bonds greatly.

As a concluding remark, we would like to highlight that these drastic changes in reactivity and basicity do arise, even though the total energy difference between $K_2Ti_4O_9$ and "$K_2NbTi_3O_9$", for example, is no larger than 1.1%. Therefore, big changes in "chemistry" may happen as a consequence of only tiny electronic perturbations.

To summarize, we have shown our *Ansatz* to *reproduce* the atomic characteristics concerning reactivity, acidity, and basicity within $K_2Ti_4O_9$. We believe that this method can be used as a tool to design solid-state chemical syntheses. Further work on solid-state reactions is in progress.

Appendix: Reactivity within a Molecule

The partitioning of a molecule's hardness η into atomic (or bonding) contributions is directly connected to quantum-chemical energy partitioning schemes that have a long history in theoretical chemistry.[55,56] These techniques have already been reviewed in detail.[57]

For molecules, the absolute hardness is given by the original two-point finite-difference formula (eq 6) of Parr and Pearson. Substituting the ionization energy and electron affinity with the energies of the LUMO and HOMO (thus directly using Koopmans' theorem[58]) leads to

$$\eta \approx \tfrac{1}{2}(-\epsilon^{+} + \epsilon^{-}) \tag{A.1}$$

$$\approx \tfrac{1}{2}(\epsilon_{\mathrm{LUMO}} - \epsilon_{\mathrm{HOMO}}) \tag{A.2}$$

If the Hamiltonian matrix elements ("hopping elements", "exchange integrals") and variational coefficients are already known, the energies of LUMO and HOMO can be expressed, using EH language[59,60] as

$$\epsilon_{\mathrm{LUMO}} = \sum_{R} \sum_{\substack{\mu \\ \mu\in R}} h_{\mu\mu} c_{\mu\mathrm{LUMO}}^{2} + \sum\sum_{R\neq R'} \sum_{\substack{\mu \\ \mu\in R}} \sum_{\substack{\nu \\ \nu\in R'}} h_{\mu\nu} c_{\mu\mathrm{LUMO}}^{*} c_{\nu\mathrm{LUMO}} \tag{A.3}$$

$$\epsilon_{\mathrm{HOMO}} = \sum_{R} \sum_{\substack{\mu \\ \mu\in R}} h_{\mu\mu} c_{\mu\mathrm{HOMO}}^{2} + \sum\sum_{R\neq R'} \sum_{\substack{\mu \\ \mu\in R}} \sum_{\substack{\nu \\ \nu\in R'}} h_{\mu\nu} c_{\mu\mathrm{HOMO}}^{*} c_{\nu\mathrm{HOMO}} \tag{A.4}$$

Both HOMO and LUMO energies incorporate a sum over all atoms R, suggesting a partitioning of the absolute hardness into local contributions. A more formal derivation which explicitly shows the effect of Koopmans' theorem can be given as follows.

In molecular orbital theory, typically the molecule's exact wave function ψ is given as the Hartree or Hartree–Fock product of one-electron wave functions ϕ_i, themselves approximated according to the Ritz variational principle by a linear combination of atomic orbitals φ_μ, as in

$$\phi_i(\vec{r}) = \sum_{R} \sum_{\substack{\mu \\ \mu\in R}} c_{\mu i} \varphi_\mu(\vec{r}) \tag{A.5}$$

Within the one-electron picture, all accessible electronic information about a molecule is given by its *density matrix* $P_{\mu\nu}$

$$P_{\mu\nu} = \sum_{i=1}^{N/2} n_i c_{\mu i}^{*} c_{\nu i} \tag{A.6}$$

for $N/2$ orbitals with occupation numbers n_i, $0 \leq n_i \leq 2$. For simplicity we assume the restricted (non-spin-polarized) case here and in the sequel. In general, the sum of all one-particle energies gives the (simplified) total energy which is equivalent to the exact total energy within EH theory according to

$$E = \sum_{i=1}^{N/2} n_i \epsilon_i \tag{A.7}$$

This can then be broken down[61] into atomic and bonding contributions

$$E = \sum_{R} E_R + \sum\sum_{R\neq R'} E_{RR'} \tag{A.8}$$

where we have made the abbreviations of "atomic energy" E_R

$$E_R = \sum_{\substack{\mu \\ \mu\in R}} P_{\mu\mu} h_{\mu\mu} \tag{A.9}$$

and "bonding energy" $E_{RR'}$

$$E_{RR'} = \sum_{\substack{\mu \\ \mu\in R}} \sum_{\substack{\nu \\ \nu\in R'}} P_{\mu\nu} h_{\mu\nu} \tag{A.10}$$

and h is the simplified one-electron Hamiltonian of EH theory. In full notation we get

$$E = \sum_{R} \sum_{\substack{\mu \\ \mu\in R}} P_{\mu\mu} h_{\mu\mu} + \sum\sum_{R\neq R'} \sum_{\substack{\mu \\ \mu\in R}} \sum_{\substack{\nu \\ \nu\in R'}} P_{\mu\nu} h_{\mu\nu} \tag{A.11}$$

$$= \sum_{R} \sum_{\substack{\mu \\ \mu\in R}} \sum_{i}^{\mathrm{HOMO}} n_i c_{\mu i}^{2} h_{\mu\mu} + \sum\sum_{R\neq R'} \sum_{\substack{\mu \\ \mu\in R}} \sum_{\substack{\nu \\ \nu\in R'}} \sum_{i}^{\mathrm{HOMO}} n_i c_{\mu i}^{*} c_{\nu i} h_{\mu\nu} \tag{A.12}$$

where the first part of the electronic energy is located on the atomic centers R while the second part is located between them, i.e., in the bonds. For simplification we rewrite the last formula as thus formally separating the states below the HOMO (whose energy contribution we called $E_{-\infty}^{\mathrm{HOMO-1}}$) from the others above (whose energy we will call E^{above}). Finally, we make the simplifying assumption that all states below the HOMO will be *unaffected*

Table VIII. EH Total Energies and Absolute Hardnesses of $K_2Ti_4O_9$, "$K_2NbTi_3O_9$", and Electronically "Modified" $K_2Ti_4O_9$

compound	electrons	E (eV)	η (eV)
$[K_2Ti_4O_9]^0$	72	−1425.030	2.545
["$K_2NbTi_3O_9$"]^0	73	−1440.572	0.130
$[K_2Ti_4O_9]^0$, (Ti(3) with Nb atomic functions)	72	−1425.624	2.357
$[K_2Ti_4O_9]^0$, (Ti(3) with Nb Coulomb integral)	72	−1428.803	2.093
$[K_2Ti_4O_9]^-$	73	−1434.442	0.110

whether higher states are occupied or not. This kind of "frozen state assumption" suppressing electronic relaxation is equivalent to the requirement of Koopmans' theorem.

Then the partitioning of the absolute hardness of the molecule into atomic and bonding contributions may easily be calculated by taking the three-point finite-difference approximation (eq 14):

$$E = E_{-\infty}^{\text{HOMO-1}} + \sum_{R}\sum_{\substack{\mu \\ \mu\in R}} n_{\text{HOMO}}c^2_{\mu\text{HOMO}}h_{\mu\mu} + \sum_{R\neq R'}\sum_{\substack{\mu \\ \mu\in R}}\sum_{\substack{\nu \\ \nu\in R'}} n_{\text{HOMO}}c^*_{\mu\text{HOMO}}c_{\nu\text{HOMO}}h_{\mu\nu} \quad \text{(A.13)}$$

$$\eta \approx \frac{1}{2}(E^+ + E^-) - E^0 \quad \text{(A.14)}$$

$$\approx \frac{1}{2}((E_{-\infty}^{\text{HOMO-1}} + E^{\text{above}})^+ + (E_{-\infty}^{\text{HOMO-1}} + E^{\text{above}})^-) - (E_{-\infty}^{\text{HOMO-1}} + E^{\text{above}})^0 \quad \text{(A.15)}$$

$$\approx \frac{1}{2}((E^{\text{above}})^+ + (E^{\text{above}})^-) - (E^{\text{above}})^0 \quad \text{(A.16)}$$

$$\approx \frac{1}{2}\Bigg(\sum_{R}\sum_{\substack{\mu \\ \mu\in R}} c^2_{\mu\text{HOMO}}h_{\mu\mu} + \sum_{R\neq R'}\sum_{\substack{\mu \\ \mu\in R}}\sum_{\substack{\nu \\ \nu\in R'}} c^*_{\mu\text{HOMO}}c_{\nu\text{HOMO}}h_{\mu\nu} + \sum_{R}\sum_{\substack{\mu \\ \mu\in R}} 2c^2_{\mu\text{HOMO}}h_{\mu\mu} + \sum_{R}\sum_{\substack{\mu \\ \mu\in R}} c^2_{\mu\text{LUMO}}h_{\mu\mu} + \sum_{R\neq R'}\sum_{\substack{\mu \\ \mu\in R}}\sum_{\substack{\nu \\ \nu\in R'}} 2c^*_{\mu\text{HOMO}}c_{\nu\text{HOMO}}h_{\mu\nu} + \sum_{R\neq R'}\sum_{\substack{\mu \\ \mu\in R}}\sum_{\substack{\nu \\ \nu\in R'}} c^*_{\mu\text{LUMO}}c_{\nu\text{LUMO}}h_{\mu\nu}\Bigg) - \sum_{R}\sum_{\substack{\mu \\ \mu\in R}} 2c^2_{\mu\text{HOMO}}h_{\mu\mu} - \sum_{R\neq R'}\sum_{\substack{\mu \\ \mu\in R}}\sum_{\substack{\nu \\ \nu\in R'}} 2c^*_{\mu\text{HOMO}}c_{\nu\text{HOMO}}h_{\mu\nu} \quad \text{(A.17)}$$

$$\approx \frac{1}{2}\Bigg(\sum_{R}\sum_{\substack{\mu \\ \mu\in R}} c^2_{\mu\text{LUMO}}h_{\mu\mu} - \sum_{R}\sum_{\substack{\mu \\ \mu\in R}} c^2_{\mu\text{HOMO}}h_{\mu\mu} + \sum_{R\neq R'}\sum_{\substack{\mu \\ \mu\in R}}\sum_{\substack{\nu \\ \nu\in R'}} c^*_{\mu\text{LUMO}}c_{\nu\text{LUMO}}h_{\mu\nu} - \sum_{R\neq R'}\sum_{\substack{\mu \\ \mu\in R}}\sum_{\substack{\nu \\ \nu\in R'}} c^*_{\mu\text{HOMO}}c_{\nu\text{HOMO}}h_{\mu\nu}\Bigg) \quad \text{(A.18)}$$

$$\approx \frac{1}{2}\sum_{R}\sum_{\substack{\mu \\ \mu\in R}}\Bigg\{h_{\mu\mu}(c^2_{\mu\text{LUMO}} - c^2_{\mu\text{HOMO}}) + \sum_{R'}\sum_{\substack{\nu \\ \nu\in R'}} h_{\mu\nu}(c^*_{\mu\text{LUMO}}c_{\nu\text{LUMO}} - c^*_{\mu\text{HOMO}}c_{\nu\text{HOMO}})\Bigg\} \quad \text{(A.19)}$$

Obviously the absolute hardness of the molecule can be decomposed into contributions of specific atoms R or specific atomic orbitals μ. Introducing an approximate *atomic reactivity increment* $\tilde{\xi}$ that fulfills the equation

$$\eta \equiv \sum_{R}\tilde{\xi}_R \quad \text{(A.20)}$$

it is easy to see that this increment arises from *difference densities* both at the atomic site and in the bonds which are *weighted* by the specific Hamiltonian matrix elements while going from the LUMO to the HOMO, i.e., as

$$\tilde{\xi}_R \approx \frac{1}{2}\sum_{\substack{\mu \\ \mu\in R}}\Bigg\{h_{\mu\mu}\Delta c^2_{\mu}(\text{LUMO} \rightarrow \text{HOMO}) + \sum_{R'}\sum_{\substack{\nu \\ \nu\in R'}} h_{\mu\nu}\Delta c_{\mu\nu}(\text{LUMO} \rightarrow \text{HOMO})\Bigg\} \quad \text{(A.21)}$$

with the abbreviations for the difference densities

$$\Delta c^2_{\mu}(\text{LUMO} \rightarrow \text{HOMO}) = c^2_{\mu\text{LUMO}} - c^2_{\mu\text{HOMO}} \quad \text{(A.22)}$$

$$\Delta c_{\mu\nu}(\text{LUMO} \rightarrow \text{HOMO}) = c^*_{\mu\text{LUMO}}c_{\nu\text{LUMO}} - c^*_{\mu\text{HOMO}}c_{\nu\text{HOMO}} \quad \text{(A.23)}$$

By comparison of these expressions with the result of the two-point finite-difference expression, the equivalency of the "frozen state approximation" with Koopmans' theorem is obvious.

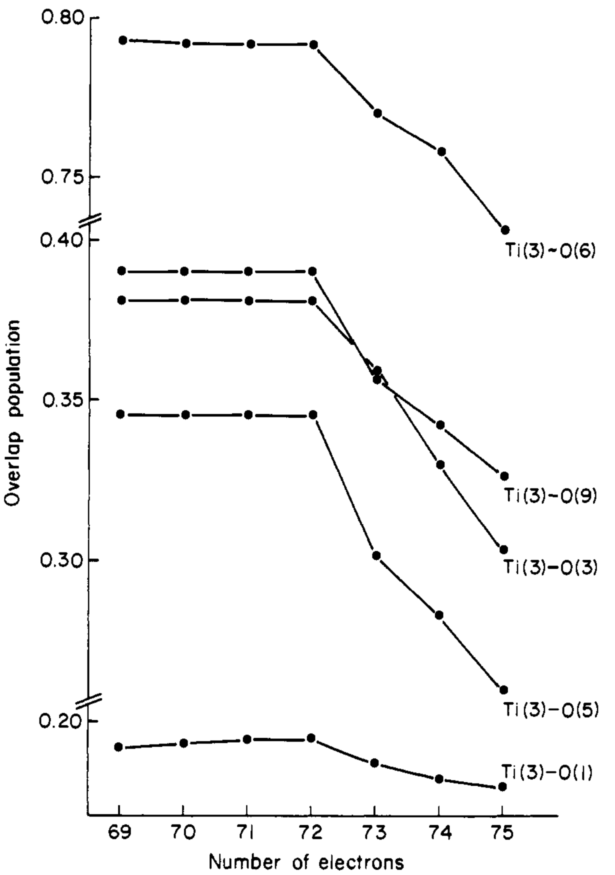

Figure 7. Integrated overlap populations up to the Fermi level of the bonds between Ti(3) and the surrounding O atoms in $K_2Ti_4O_9$ as a function of the valence electron count.

Acknowledgment. First of all, the author wants to express his gratitude to Professor Roald Hoffmann for his hospitality and his initial inducement to set up acid–base descriptors for the solid state. Furthermore, he supported the present work with critical remarks, instructive suggestions, and supply of computation time on Cornell's computer network. In addition, the author wants to thank Professor Jean Rouxel both for an inspiring discussion on "soft chemistry" at the Baker laboratory in spring 1991, as well as for sending some preprints about acid–base solid-state chemistry. The financing of the author's and his family's life in Ithaca (NY) by the Liebig scholarship of the Verband der Chemischen Industrie (Germany) is gratefully acknowledged. Also, it is a pleasure to thank Jane Jorgensen for the beautiful drawings.

Registry No. O, 17778-80-2.